Clim. Past Discuss., https://doi.org/10.5194/cp-2019-25
Manuscript under review for journal Clim. Past
Discussion started: 4 March 2019

Climate of the Past
Discussions
Open Access
EGU

Evaluating model outputs using integrated global speleothem records of climate change since the last glacial

Laia Comas-Bru[1,2,*], Sandy P. Harrison[1], Martin Werner[3], Kira Rehfeld[4], Nick Scroxton[5], Cristina Veiga-Pires[6] and SISAL working group members

Corresponding author: Laia Comas-Bru (l.comasbru@reading.ac.uk)

1- School of Archaeology, Geography & Environmental Sciences, Reading University, Whiteknights, Reading, RG6 6AH, UK
2- UCD School of Earth Sciences. University College Dublin, Belfield. Dublin 4, Ireland.
3- Alfred Wegener Institute. Helmholtz Centre for Polar and Marine Research. Division Climate Science - Paleoclimate Dynamics. Bussestr. 24, D-27570 Bremerhaven, Germany
4- Institute of Environmental Physics, Ruprecht-Karls-Universität Heidelberg, Im Neuenheimer Feld 229, 69120 Heidelberg, Germany
5- Department of Geosciences, University of Massachusetts Amherst, 611 North Pleasant Street, 01003-9297 Amherst, MA, USA
6- Universidade do Algarve Faculdade de Ciências do Mar e do Ambiente - FCMA Centro de Investigação Marinha e Ambiental - CIMA Campus de Gambelas 8005-139 Faro Portugal

Clim. Past Discuss., https://doi.org/10.5194/cp-2019-25
Manuscript under review for journal Clim. Past
Discussion started: 4 March 2019

Climate of the Past Discussions

Abstract: Although quantitative isotopic data from speleothems has been used to evaluate isotope-enabled model simulations, currently no consensus exists regarding the most appropriate methodology through which achieve this. A number of modelling groups will be running isotope-enabled palaeoclimate simulations in the framework of the Coupled Model Intercomparison Project Phase 6, so it is timely to evaluate different approaches to use the speleothem data for data-model comparisons. Here, we accomplish this using 456 globally-distributed speleothem $\delta^{18}O$ records from an updated version of the Speleothem Isotopes Synthesis and Analysis (SISAL) database and palaeoclimate simulations generated using the ECHAM5-wiso isotope-enabled atmospheric circulation model. We show that the SISAL records reproduce the first-order spatial patterns of isotopic variability in the modern day, strongly supporting the application of this dataset for evaluating model-derived isotope variability into the past. However, the discontinuous nature of many speleothem records complicates procuring large numbers of records if data-model comparisons are made using the traditional approach of comparing anomalies between a control period and a given palaeoclimate experiment. To circumvent this issue, we illustrate techniques through which the absolute isotopic values during any time period could be used for model evaluation. Specifically, we show that speleothem isotope records allow an assessment of a model's ability to simulate spatial isotopic trends and the degree to which the model reproduces the observed environmental controls of isotopic spatial variability. Our analyses provide a protocol for using speleothem isotopic data for model evaluation, including screening the observations, the optimum period for the modern observational baseline, and the selection of an appropriate time-window for creating means of the isotope data for palaeo time slices.

1. Introduction

Earth System Models (ESMs) are routinely used to project the consequences of current and future anthropogenic forcing of climate, and the impacts of these projected changes on environmental services (e.g., Christensen et al., 2013;Collins et al., 2013;Kirtman et al., 2013;Field, 2014). ESMs are routinely evaluated using modern and historical climate data. However, the range of climate variability experienced during the period for which we have reliable historic climate observations is small, much smaller than the amplitude of changes projected for the 21st century. Radically different climate states in the geologic past provide an opportunity to test the performance of ESMs in response to very large changes in forcing, changes that in some cases are as large as the expected change in forcing at the end of the 21st century (Braconnot et al., 2012). The use of "out-of-sample" testing (Schmidt et al., 2014) is now part of the evaluation procedure of the Coupled Model Intercomparison Project (CMIP). Several palaeoclimate simulations are being run by the Palaeoclimate Modelling Intercomparison Project (PMIP) as part of the sixth phase of CMIP (CMIP6-PMIP4), including simulations of the Last Millennium (LM, 850–1850 CE, *past1000*), mid-Holocene (MH, ca. 6000 yrs BP, *midHolocene*) Last Glacial Maximum (LGM, ca. 21,000 yrs BP, *lgm*), the Last Interglacial (LIG, ca. 127,000 yrs BP, *lig127k*) and the mid-Pliocene Warm Period (mPWP, ca. 3.2 M yrs BP, *midPliocene-eoi400*) (Kageyama et al., 2017).

Although these CMIP6-PMIP4 time periods were selected because they represent a range of different climate states, the choice also reflects the fact that global syntheses of palaeoenvironmental and palaeoclimate observations exist across them, thereby providing the opportunity model benchmarking (Kageyama et al., 2017). However, both the geographic and temporal coverage of the different types of data is uneven. Ice core records are confined to polar and high-altitude regions and provide regionally to globally integrated signals of forcings and climatic responses. Marine records provide a relatively comprehensive coverage of the ocean state for the LGM, but low rates of sedimentation mean they are less informative about the more recent past (Hessler et al., 2014). Lake records provide qualitative information of terrestrial hydroclimate, but the most comprehensive source of quantitative climate information over the continents is based on statistical calibration of pollen records (see e.g., Bartlein et al., 2011). However, pollen preservation requires the long-term accumulation of sediments under anoxic conditions and is consequently limited in semi-arid, arid and highly dynamic wet regions such as in the tropics.

Oxygen isotopic records ($\delta^{18}O$) from speleothems, secondary carbonate deposits that form in caves from water that percolates through carbonate bedrock (Atkinson, 1977;Fairchild and Baker, 2012), provide an alternative source of information about past terrestrial climates. Although there are hydroclimatic limits on the growth of speleothems, their distribution is largely constrained by the existence of suitable geological formations and they are found growing under a wide range of climate conditions, from extremely cold climates in Siberia (Vaks et al., 2013) to arid regions of Australia (Treble et al., 2017). Therefore, speleothems have the potential to provide information about past terrestrial climates in regions for which we do not have (and are unlikely to have) information from pollen. As is the case with pollen, where quantitative climate reconstructions must be obtained through statistical or forward modelling approaches (Bartlein et al., 2011), the interpretation of speleothem isotope records in terms of climate variables is in some cases not straightforward (Fairchild and Baker, 2012;Lachniet, 2009). However, some ESMs now use water isotopes as tracers for the diagnosis of hydroclimate (Werner et al., 2016;Tindall et al., 2009;Schmidt et al., 2007), and this opens up the possibility of using speleothem isotopic measurements directly for comparison with model outputs. At least six modelling groups are planning isotope-enabled palaeoclimate simulations as part of CMIP6-PMIP4.

As with other model evaluation studies, much of the diagnosis of isotope-enabled ESMs has focused on modern day conditions (e.g., Joussaume et al., 1984;Hoffmann et al., 1998;Noone and Simmonds, 2002;Schmidt et al., 2007;Roche, 2013;Xi, 2014;Risi et al., 2016;Hu et al., 2018;Jouzel et al., 2000;Hoffmann et al., 2000). However, isotope-enabled models have also been used in a palaeoclimate context (e.g., Schmidt et al., 2007;LeGrande and Schmidt, 2008;LeGrande and Schmidt, 2009;Caley and Roche, 2013;Caley et al., 2014;Jasechko et al., 2015;Werner et al., 2016;Langebroek et al., 2011;Zhu et al., 2017). The evaluation of these simulations has often focused on isotope records from polar ice cores and from marine environments. Where use has been made of speleothem records, the comparison has generally been based on a relatively small number of the available records. Furthermore, all of the comparisons make use of an empirically-derived correction for the

Clim. Past Discuss., https://doi.org/10.5194/cp-2019-25
Manuscript under review for journal Clim. Past
Discussion started: 4 March 2019

Climate of the Past Discussions
Open Access

temperature-dependence fractionation of calcite $\delta^{18}O$ at the time of speleothem formation that is based on synthetic carbonates (Kim and O'Neil, 1997). This fractionation is generally poorly constrained (McDermott, 2004;Fairchild and Baker, 2012), does not account for any non-equilibrium of kinetic fractionation at the time of deposition and is not suitable for aragonite samples. Thus, using a single standard correction and not screening records for mineralogy introduces uncertainty into the data-model comparisons.

SISAL (Speleothem Isotopes Synthesis and Analysis), an international working group under the auspices of the Past Global Changes (PAGES) project (http://pastglobalchanges.org/ini/wg/sisal), is an initiative to provide a reliable, well-documented and comprehensive synthesis of isotopic records from speleothems worldwide (Comas-Bru and Harrison, 2019). The first version of the SISAL database (SISALv1: Atsawawaranunt et al., 2018a;Atsawawaranunt et al., 2018b) included 381 speleothem-based isotope records and metadata to facilitate quality control and record selection. A major motivation for the SISAL database was to provide a tool for benchmarking of palaeoclimate simulations using isotope-enabled models.

In this paper, we examine a number of issues that need to be addressed in order to use the SISAL data for model evaluation in the palaeoclimate context and make recommendations about robust approaches that should be used for model evaluation in CMIP6-PMIP4. We focus on the MH and LGM time periods, partly because the *midHolocene* and *lgm* experiments are the “entry cards” for the CMIP6-PMIP4 simulations and partly because these are the PMIP time periods with the best coverage of speleothem records. We use an updated version of the SISAL database (SISALv1b: Atsawawaranunt et al., 2019) and simulations made with the ECHAM5-wiso isotope-enabled atmospheric circulation model (Werner et al., 2011) to explore the various issues in making data-model comparisons.

Section 2 introduces the data and the methods used in this study. Section 2.1 introduces the isotope-enabled model simulations for the modern (1958–2013), the *midHolocene* and the *lgm* experiments, explains the methods used to calculate weighted simulated $\delta^{18}O$ values, and provides information about the construction of time-slices. Section 2.2 presents the modern observed $\delta^{18}O$ in precipitation ($\delta^{18}O_p$) used. Section 2.3 introduces the speleothem isotopic data from the SISAL database and explains the rationale for screening records. Section 3 describes the results of the analyses, specifically the spatio-temporal coverage of the SISAL records (Section 3.1), the representation of modern conditions (Section 3.2), anomaly-mode time-slice comparisons (Section 3.3), and the comparison of $\delta^{18}O$ gradients in absolute values along spatial transects to test whether the model accurately records regional variations in $\delta^{18}O$ (Section 3.4). Section 4 provides a protocol for using speleothem isotopic records for data-model comparisons and section 5 summarises our main conclusions.

2. Methods

2.1. Model simulations

ECHAM5-wiso (Werner et al., 2011) is the isotope-enabled version of the ECHAM5 atmosphere GCM (Roeckner et al., 2003;Roeckner et al., 2006;Hagemann et al., 2006). The water cycle in ECHAM5 contains formulations for evapotranspiration of terrestrial water, evaporation of ocean water, and the formation of large-scale and convective clouds. Vapour, liquid, and frozen water are transported independently within the atmospheric advection scheme. The stable water isotope module in ECHAM5 computes the isotopic signal of different water masses through the entire water cycle, including in precipitation and soil water.

ECHAM5-wiso was run for 1958–2013, using an implicit nudging technique to constrain simulated fields of surface pressure, temperature, divergence and vorticity to the corresponding ERA-40 and ERA-Interim reanalysis fields (Butzin et al., 2014). The *midHolocene* simulation (Wackerbarth et al., 2012) was forced by orbital parameters and greenhouse gas concentrations appropriate to 6 ka following the PMIP3 protocol (https://pmip3.lsce.ipsl.fr). The control simulation has modern values for the orbital parameters and greenhouse gas (GHG) concentrations (Wackerbarth et al., 2012). The change in sea surface temperatures (SST) and sea ice cover between 6 ka and the pre-industrial period were calculated from 50-year averages from each interval extracted from a transient Holocene simulation performed with the fully coupled ocean-atmosphere Community Climate System Model CCSM3 (Collins et al., 2006). The anomalies were then added to the observed modern SST and sea ice cover data to force the *midHolocene* simulation (Wackerbarth et al., 2012). For the *lgm* experiment (Werner et al., 2018), orbital parameters, GHG concentrations, land-sea distribution, and ice sheet height and extent followed the PMIP3 guidelines. Climatological monthly sea ice coverage and SST changes were prescribed from the GLAMAP dataset (Paul and Schäfer-Neth, 2003). A uniform glacial enrichment of sea surface water and sea ice of +1‰ ($\delta^{18}O$) and +8‰ (δD) on top of the present-day isotopic composition of surface seawater was applied. For the ocean surface sate of the corresponding control simulation, monthly climatological SST and sea ice cover for the period 1979-1999 were prescribed. All the ECHAM5-wiso simulations were run at T106 horizontal grid resolution (approx. 1.1°x1.1°) with 31 vertical levels. The *midHolocene* and *lgm* experiments were run for 12 and 22 years, respectively. Model anomalies for the MH and the LGM were calculated as the differences between the MH/LGM simulation and the corresponding control simulations. We also calculated the anomaly between the LGM and MH (LGM-MH), taking account of the difference between their control simulations. We constructed simulated isotope anomalies by averaging the last 10 (*midHolocene*) and 20 (*lgm*) years of the simulations.

At best, the speleothem isotopic signal will be an average of the precipitation $\delta^{18}O$ ($\delta^{18}O_p$) signals weighted towards those months when precipitation is greatest. However, the signal is transmitted via the karst system, and is therefore modulated by storage in the soil, recharge rates, mixing in the subsurface, and varying residence times - ranging from hours to years (e.g. Breitenbach et al., 2015;Riechelmann et al., 2017). These factors could all exacerbate differences between observations and simulations. We investigated whether weighting the simulated $\delta^{18}O$ signals by soil moisture or recharge amount provided a better comparison measure than weighting by precipitation amount by calculating three indices: (i) $\delta^{18}O_p$ weighted according to monthly precipitation amount ($w\delta^{18}O_p$); (ii) $\delta^{18}O_p$ weighted according to the potential recharge amount calculated as precipitation minus evaporation (P-E) for months where P-E > 0 (w$\delta^{18}O_{recharge}$); and (iii) soil water δ^{18}O weighted according to soil moisture amount (w$\delta^{18}O_{sw}$). To investigate the impact of transit time on the comparisons, we smoothed the simulated wδ^{18}O using a range of smoothing from 1–20 years. Finally, we investigated whether differences in elevation between the model grid and speleothem records had an influence on the quality of the data-model comparisons by applying an elevational correction of -2.5‰/km (Lachniet, 2009) to the simulated wδ^{18}O.

2.2. Modern observations

We use two sources of modern isotope data for assessment purposes: (i) $\delta^{18}O_p$ measurements from the Global Network of Isotopes in Precipitation (GNIP) database (IAEA/WMO, 2018) and (ii) a gridded dataset of global water isotopes from the Online Isotopes in Precipitation Calculator (OIPC: Bowen, 2018;Bowen and Revenaugh, 2003).

The GNIP database provides raw monthly $\delta^{18}O_p$ values for some part of the interval 03/1960 to 08/2017 for 977 stations. Individual stations have data for different periods of time and there are gaps in most individual records; only two stations have continuous data for over 50 years and both are in Europe (Valentia Observatory, Ireland, and Vienna Hohe-Warte, Austria). Most GNIP stations are more than 0.5° away from the SISAL cave sites, precluding a direct global comparison between GNIP and SISAL records. However, the GNIP data can be used to examine simulated interannual variability. Annual δ^{18}O averages were calculated from GNIP stations with at least 10 months of data per year and 5 or more years of data. Annual $\delta^{18}O_p$ data was extracted from the ECHAM5-wiso simulations at the location of the GNIP stations for the years for which GNIP data is available at each station. We exclude GNIP stations from coastal locations that are not land in the ECHAM5-wiso simulation. This dual screening results in only 450 of the 977 GNIP stations being used for comparisons. Boxplots are calculated with the standard deviation of annual $\delta^{18}O_p$ data.

Clim. Past Discuss., https://doi.org/10.5194/cp-2019-25
Manuscript under review for journal Clim. Past
Discussion started: 4 March 2019

Climate of the Past Discussions
Open Access
EGU

The OIPC dataset provides a gridded long-term global (1960–2017) record of modern w$\delta^{18}O_p$, based on combining data from 348 GNIP stations covering part or all the period 1960–2014 (IAEA/WMO, 2017) and other w$\delta^{18}O_p$ records from the Water Isotopes Database (Waterisotopes Database, 2017). The OIPC data can be used to evaluate spatial patterns in both the SISAL records and the simulations.

2.3. Speleothem isotope data

We use an updated SISAL database (SISALv1b: Atsawawaranunt et al., 2019), which provides revised versions of 45 records from SISALv1 and includes 60 new records (Table 1). SISALv1b has isotope records from 455 speleothems from 211 cave sites distributed worldwide. Because the isotopic fractionation between water and $CaCO_3$ differs between calcite and aragonite, we only use calcite speleothems or aragonite speleothems where the correction to calcite values was made by the original authors for simplicity. However, using the reformulated aragonite $\delta^{18}O$-water equation of Grossman and Ku (1986) from Lachniet (2015) would allow the incorporation of the currently small number of aragonite records from the SISAL database to the data-model comparison. As a result of this screening, we use 370 speleothem records from 174 cave sites for comparisons. However, the number of speleothem records covering specific periods (i.e., modern, MH, LGM) is considerably lower.

Recent data suggests that many calcite speleothems are precipitated out of isotopic equilibrium with waters (Daëron et al., 2019). Therefore, we have converted SISAL data to its drip-water equivalent using an empirical speleothem-based fractionation factor that accounts for any non-equilibrium of kinetic fractionation that may arise in the precipitation of calcite speleothems in caves (Tremaine et al., 2011). We use the V-PDB to V-SMOW conversion from Coplen et al. (1983) (as in Sharp, 2007).

$$\delta^{18}O_{calcite\_SMOW} = 0.97002 \cdot \left(\delta^{18}O_{calcite\_PDB} + 29.98\right)$$

$$\delta^{18}O_{dripw\_SMOW} = \delta^{18}O_{calcite\_SMOW} - \left(\left(\frac{16.1 \cdot 1000}{T}\right) - 24.6\right) \quad \text{(T in K)}$$

Clim. Past Discuss., https://doi.org/10.5194/cp-2019-25
Manuscript under review for journal Clim. Past
Discussion started: 4 March 2019

Climate of the Past Discussions

We have used mean annual surface air temperature from CRU-TS4.01 (Harris et al., 2014) for the OIPC comparison and ECHAM5-wiso simulated mean annual temperature for the SISAL-model comparison as a surrogate of modern and past cave air temperature (Moore and Sullivan, 1997) Uncertainties are introduced in this conversion from several unknown factors such as cave temperature and pCO_2 of soil.

We compare the modern temporal variability in the SISAL records with ECHAM5-wiso by extracting simulated w$\delta^{18}O_p$ at the cave site location for all the years for which there are speleothem isotope samples. The speleothem isotope ages were rounded to exact calendar years for this comparison.

Data-model comparisons are generally made by comparing anomalies between a control period and a palaeoclimate simulation with data anomalies with respect to a modern baseline. There is no agreed standard defining the interval used as a modern baseline for palaeoclimate reconstructions. Some studies have used modern observational datasets which cover a specific and limited period of time and some use the late 20th century as a reference. We investigate the appropriate choice of modern baseline for the speleothem records by comparing the interval centred on 1850 CE with alternative intervals covering the late 20th century, specifically 1961-1990 and 1850–1990 CE, and we assess the impact of these choices on both mean $\delta^{18}O$ values and the number of records available for comparison. The MH time slice was defined as 6,000 ±500 yrs BP (where present is 1950 CE) and the LGM time slice as 21,000 ±1,000 yrs BP, following the conventional definitions of these intervals used in the construction of other benchmark palaeoclimate datasets (e.g., MARGO project members, 2009;Bartlein et al., 2011). However, we also examined the impact of using shorter intervals for each time slice. In addition to calculating LGM and MH anomalies with respect to modern, we also calculated the anomaly between the LGM and MH (LGM-MH).

We use the published age-depth models for each speleothem record. There is no information about the temporal uncertainties on individual isotope samples for most of the records in SISALv1b. This precludes a general assessment of the impact of temporal uncertainties on data-model comparisons.

We assess these impacts for the LGM for two records (entity BT-2 from Botuverá cave: Cruz et al., 2005;and entity SSC01 from Gunung-buda cave: Partin et al., 2007) for which new age-depth models have been prepared using COPRA (Breitenbach et al., 2012). We created 1,000-member ensembles of the age-depth relationship using the original author's choice of radiometric dates and *pchip* interpolation. Isotope ratio means were calculated using time windows of increasing width (100 to 3,000 years) around 21 kyrs BP for the original age-depth model, the COPRA median age model, and all ensemble members. All COPRA-based uncertainties have been projected to the chronological axes.

To explore the use of absolute isotopic data for model evaluation, we extracted absolute data for six transects illustrating key features of MH and LGM geographic isotopic patterns. The MH transects run from NW to SE across America, NW to SE across SE Asia, and N-S across southern Europe and northern Africa. The LGM transects run N-S from central Europe to southern Africa, from NW to SE in America, and N-S from China to northern Australia. Each transect follows the great circle line between two locations. The longitudinal span of each transect varies to maximise the number of SISAL records included. We extracted model outputs for the same transects, using the model land/sea mask to remove ocean grid cells. The simulated absolute values were extracted along the great circle lines at 1.12° steps to match the model grid size. Comparisons are made between the SISAL mean $\delta^{18}O$ value and the simulated $w\delta^{18}O_p$ values averaged within a longitudinal range. We also compare simulated mean annual surface air temperature (MAT) and mean annual precipitation (MAP) with pollen-based quantitative reconstructions of MAT and MAP from Bartlein et al. (2011). The pollen-based anomalies have been converted to absolute values by adding the CRU-TS4.01 climatology (Harris et al., 2014).

Speleothem growth is inhibited in very dry climates, so the presence/absence of speleothems has been interpreted as a direct indication of climate state (Gascoyne et al., 1983;Vaks et al., 2006;Vaks et al., 2013). Speleothem distribution through time approximates an exponential curve in many regions around the world (e.g., Ayliffe et al., 1998;Jo et al., 2014;Scroxton et al., 2016). This relationship suggests that the natural attrition of stalagmites is independent of the age of the specimens and approximately constant through time, despite potential complications from erosion, climatic changes and sampling bias. The underlying exponential curve can, therefore, be thought of as a prediction of the number of expected stalagmites given the existing population. Intervals when climate conditions were more/less favourable to speleothem growth can then be identified from changes in the population size by subtracting this underlying exponential curve (Scroxton et al., 2016). We apply this approach at a global level to the unscreened SISAL data by counting the number of individual caves with stalagmite growth during every 1,000-yr period from 500 kyrs BP to the present. Growth was indicated by a stable isotope sample at any point in each 1,000-year bin, giving 3,866 data points distributed in 500 bins. We use cave numbers, rather than the number of individual speleothems, to minimise the risk of over-sampled caves influencing the results. Random resampling (100,000) of the 3,866 data points was used to derive 95% and 5% confidence intervals. The number of speleothems cannot be reliably predicted by a continuous distribution when numbers are low, so we do not consider intervals prior to 266 kyrs BP – the most recent interval with less than four records.

3. Results

3.1. Spatial and temporal coverage of speleothem records

There are many regions of the world where the absence of carbonate lithologies means that there will never be speleothem records (Fig. 1a). Nevertheless, SISALv1b represents a substantial improvement in spatial coverage compared to SISALv1, particularly for Australasia and Central and North American (Fig. 1a, Table 1), and the sampling for regions such as Europe and China is quite dense. Thus, SISALv1b provides a sufficient coverage to allow the data to be used for model evaluation. The temporal distribution of records is uneven, with only ca. 40 at 21 kyrs increasing to > 100 records at 6 kyrs and > 110 for the last 1,000 yrs (Fig. 1b). A pronounced regional bias exists towards Europe during the Holocene. Regional coverage is relatively even during the LGM, with the exception of Africa which is under-represented throughout (< 4% of total). Nevertheless, there is sufficient coverage to facilitate data-model comparisons for the MH and LGM for most regions of the world.

The global occurrence of speleothems through time approximates an exponential distribution (Fig. 2 a, b). Anomalously high numbers of speleothems are found in the last 12 kyrs, between 128–112 kyrs BP and during interglacials MIS 1 and 5e (and the early glacial MIS 5d). There are fewer than expected speleothems between 73–63 kyrs BP and during MIS 2. These deviations could arise from sampling biases but may also reflect globally wetter or drier intervals. Differences between curves constructed for tropical and temperate regions (Fig. 2 c, d) suggest these deviations are climatic in origin because there is less variability in the tropical than the temperate curve. Thus, even at a global level, the speleothem data provide a first-order assessment of climate changes on orbital time scales.

3.2. How well do the speleothem records represent modern $\delta^{18}O$ in precipitation?

The first-order spatial patterns shown by the SISAL speleothem records during the modern period (1960–2017; n = 72) are in overall agreement with the OIPC dataset of interpolated $w\delta^{18}O_p$ ($R^2 = 0.78$), with more negative values at higher latitudes and in more continental climates (Fig. 3a) as shown by McDermott et al. (2011) for European stalagmites. Low latitude sites tend to show more positive $\delta^{18}O$ values than the OIPC data, whereas sites from the mid to high-latitudes tend to be more negative (Fig. 3b). A similar bias is observed in the comparison between SISAL and the simulated $w\delta^{18}O_p$ ($R^2 = 0.79$), although in this case the slope is steeper (Fig. 3 c, d). Some discrepancies between the SISAL data and the observations or simulations may be due to cave specific factors such as a preferred seasonality of recharge, non-equilibrium fractionation processes during speleothem deposition or by complex soil-atmosphere interactions affecting evapotranspiration and, thus, the isotopic signal of the effective recharge. However, the overall level of agreement suggests that the SISAL data provide a good representation of the impacts of modern hydroclimatic processes.

Comparison of the SISAL records with $\delta^{18}O_p$ weighted according to the potential recharge amount or with $\delta^{18}O_{sw}$ weighted to the moisture amount does not significantly improve the data-model comparison (Supplementary Fig. 1). The best relationship is obtained with $w\delta^{18}O_{sw}$ ($R^2 = 0.80$). However, smoothing the simulated $w\delta^{18}O_p$ records on a sample-to-sample basis to account for multiyear transit times in the karst environment produces a slightly better geographic agreement with the SISAL records (Supplementary Fig. 2). Accounting for differences between the model grid cell and cave elevations does not yield any overall improvement in the global correlations.

Simulated inter-annual variability is less than shown in the GNIP data (Fig. 4). Although there are missing values for the GNIP station data, we have also removed these intervals from the simulations, so incomplete sampling is unlikely to explain the difference between the observed and simulated inter-annual variability. The inter-annual variability of the modern speleothem records is lower than both the simulated and the GNIP data, reflecting the impact of within karst and cave processes that effectively act as a low-pass filter on the signal recorded during speleothem growth. Smoothing the simulated $\delta^{18}O_p$ signal produces a better match to the SISAL records: application of a smoothing window of > 5 yrs to simulated w$\delta^{18}O_p$ produces a good match (95% confidence) with the inter-annual variability shown by the speleothems (Fig. 4). The fact that the temporal smoothing of the simulations produces a better match both in terms of geographic patterns and inter-annual variability results from the tendency of speleothem records to predominantly contain low-frequency information (Baker et al., 2013) and indicates that data-model comparisons using speleothem records should focus on quasi-decadal or longer timescales.

3.3. Anomaly-mode time-slice comparisons

The selection of a modern or pre-industrial base period is a first step in reconstructing speleothem $\delta^{18}O$ anomalies for comparisons with simulated changes in specific model experiments. There are 62 speleothem records that cover the pre-industrial interval 1850±15 CE, commonly used as a reference in model experiments. However, using this short interval as the base period for comparisons with MH or LGM simulations would result in the reconstruction of anomalies for only 18 records for the MH and only 5 records for the LGM - which are the number of speleothem records with isotopic samples in both the base period and either the MH or LGM (Table 2). There is no significant difference in the mean $\delta^{18}O$ values for this pre-industrial period and the modern $\delta^{18}O$ values (R^2 = 0.96; Supplementary

Clim. Past Discuss., https://doi.org/10.5194/cp-2019-25
Manuscript under review for journal Clim. Past
Discussion started: 4 March 2019

Climate of the Past Discussions

Fig. 3). Using an extended modern baseline (1850–1990 CE) increases the data uncertainties by only ±0.5‰ but raises the number of MH records for which MH-modern anomalies can be calculated to 34 entities from 29 sites around the world. There is also an improvement in the number of LGM sites for which it is possible to calculate anomalies, from 5 to 11 entities at 10 sites. Although longer base periods have been used for data-model comparisons, for example the last 1,000 years (e.g., Werner et al., 2016), this would increase the uncertainties in the observations without substantially increasing the number of records for which it would be possible to calculate anomalies, particularly for the LGM (Table 2). We, therefore, recommend the use of the interval 1850–1990 CE as the baseline for calculation of $\delta^{18}O$ anomalies from the speleothem records.

A relatively good agreement exists between the sign of the simulated and observed $\delta^{18}O$ changes at the MH and LGM: 77% of the MH entities and 64% of the LGM entities show changes in the same direction after allowing for an uncertainty of ±0.5‰ (Fig. 5 a, b). However, the magnitude of the changes is larger in the SISAL records than the simulations. The MH-modern speleothem anomalies range from -3.63 to 1.28‰ (mean±std: -0.58±1.01‰), but the simulated anomalies only range from -1.03 to 0.30‰ (mean±std: -0.13±0.31‰). Observed anomalies are 5–20 times larger than simulated anomalies in the Asian monsoon region, and in individual sites in North and South America and Uzbekistan (Fig. 5 a). The data-model mismatch is smallest in Europe, with a mean offset of 0.24±0.40‰ (n = 9 entities from 7 sites). Multivariate analyses (Supplementary Information) also show that there is no significant relationship between observed and simulated $\delta^{18}O$ patterns in the MH. A two-tailed Student t-test shows that most of the simulated anomalies are not significantly different from present (at 95% confidence). This may reflect the fact that the *midHolocene* simulation was only run for 10 years but is also consistent with previous studies which show that climate models substantially underestimate the magnitude of MH changes (Harrison et al., 2014), particularly in monsoon regions (e.g., Perez-Sanz et al., 2014).

The simulated changes in $\delta^{18}O$ at the LGM are much larger than those simulated for the MH and are significant (at 95% confidence) over much of the globe. There is no regionally coherent pattern in the observed LGM anomalies because of the limited number of speleothems that grew continuously from the LGM to present. However, the sign of the observed changes is coherent with the simulated change in $\delta^{18}O$ for 7 of the 11 records (Fig. 5 b). The magnitude of the LGM anomalies differs by less than 1‰ between model and data in half of the locations. A strong offset is found in the two records from Sofular Cave, which are ca. 6‰ more negative than the simulated $\delta^{18}O$. This offset may be related to the glacial changes in the Black Sea region, which are not well represented in the *lgm* simulation. Thus, although overall the comparison with the speleothem records suggests that the simulated changes in hydroclimate are reasonable, the simulated changes in the Middle East differ from observations. However, multivariate analyses (Supplementary Information) reveal no significant relationship between observed and simulated LGM $\delta^{18}O$ patterns.

An alternative approach to examine the realism of simulated changes is to compare the LGM and MH simulations directly, which improves the number of records for which anomalies can be calculated (Fig. 5 c; n = 20). However, the pattern of change is similar to the LGM-modern anomalies. The simulated and observed direction of change is coherent at 80% of the locations with an offset smaller than 1‰ occurring in 7 sites and again the largest discrepancy is Sofular Cave. Thus, in this particular example, a direct comparison of the LGM-MH anomalies does not provide additional insight to the comparison of LGM-modern anomalies. Nevertheless, such an approach might be useful for other time periods (e.g., comparison of early versus mid-Holocene) when there are likely to be many more speleothem records available.

Age uncertainties inherent to the speleothem samples selected to represent the LGM could partially explain the LGM data-model mismatches. A global assessment of the impact of time-window width on the MH and LGM anomalies shows that reducing the window width from ±500 to ±200 years in the MH has little impact on the average values (Supplementary Fig. 4) but reduces the inter-sample variability and produces a better match to the simulated anomalies. A similar analysis for the LGM (Supplementary Fig. 5) suggests that a window-width of ±500 years (rather than ±1,000 years) would be the most appropriate choice for comparisons of this interval. The number of SISAL sites available for such comparisons is not affected. However, analyses of the relative error of the isotope anomalies calculated at individual sites for different LGM window widths (Fig. 6) show a clear increase in all relative error components as window size decreases for BT-2 but no clear changes in the relative error terms for SSC01 (the samples from Botuverá and Gunung-buda cave, respectively, with new COPRA-produced age-depth models). These results suggest that, with an LGM window width of ±1,000 years, the relative contribution of age uncertainty to the anomaly uncertainty is small (Fig. 6). Thus, although it is clear that it would be useful to propagate age uncertainties for individual sites, changing the conventional definitions of the MH and LGM time slices in deriving speleothem anomalies does not seem warranted at this stage.

3.4. Analysis of spatial gradients

The number of sites available in SISALv1b means that quantitative data-model comparisons using the traditional anomaly approach are limited in scope. Approaches based on comparing trends in absolute $\delta^{18}O$ values could provide a way of increasing the number of observations and an alternative way to evaluate the simulations. Comparison of trends places less weight on anomalous sites and allows large-scale systematic similarities and dissimilarities between model and observations to be revealed. We illustrate this approach using spatial gradients in the MH and LGM, although such an approach could also be used for temporal trends.

The first-order trends in observed $\delta^{18}O$ changes during the MH are broadly captured by the model (Fig. 7). The largest mismatches between the observations and simulations, in the high latitudes of North America, in mid-latitude Europe and in the monsoon region of Asia, are in regions where the model does not reflect the reconstructed MAP. This confirms the suggestion, based on comparison of the MH mapped patterns (section 3.3), that ECHAM5-wiso underestimates changes in precipitation between the MH and the present day. The observed latitudinal $\delta^{18}O$ gradients in the LGM are reasonably well captured by the simulations (Fig. 8), reflecting the strong latitudinal control on $\delta^{18}O$ variability (Dansgaard, 1964). As is the case in the MH, the largest discrepancies occur in regions where the model overestimates MAP. However, this mismatch may partly reflect the fact that the pollen-based reconstructions do not take account of the low atmospheric CO_2 concentration during the glacial and, may consequently underestimate the actual precipitation amount (Prentice et al., 2017). Nevertheless, these examples show the potential to use trends in absolute values for model evaluation and diagnosis.

4. Protocol for data-model comparison using speleothem data

Our analyses illustrate a number of possible approaches for utilising use speleothem isotopic data towards model evaluation. The discontinuous nature of most speleothem records means that the number of sites available for conventional anomaly-mode comparisons is potentially limited. To some extent this is mitigated by the fact that differences between the modern and pre-industrial isotope values are small, permitting the calculation of anomalies using a longer baseline interval (1850–1990 CE). The use of smaller intervals of time in calculating MH or LGM anomalies (Supplementary Fig. 4 and 5) does not have a significant impact either on the mean values or the number of records provided the interval is > ±300 yrs for the MH and > ±500 yrs for the LGM. Although the use of shorter intervals is possible, we recommend using the conventional definitions of each time slice to facilitate comparison with other benchmark datasets. Although patterns in the isotopic anomalies can provide a qualitative assessment of model performance, site-specific factors could lead to large differences from the simulations at individual locations. Improved spatial coverage would allow such sites to be identified and screened out before making quantitative comparisons of observed and simulated anomalies. More records are available for the MH or LGM alone than for both that period (i.e. MH or LGM) and the modern baseline period, encouraging examination of spatial gradients in absolute $\delta^{18}O$. Even when an offset between the observed and simulated $\delta^{18}O$ exists, comparing the trends along such gradients is possible. Thus, both absolute values and anomalies of the isotope data for data-model comparison are useful.

Screening of published speleothem isotopic data is essential to produce meaningful data-model comparisons. The SISAL database facilitates screening for mineralogy, which has a substantial effect on isotopic values because of differences in water-carbonate fractionation factors for aragonite or calcite. We recommend the use of the empirical speleothem-based fractionation factor of Tremaine et al. (2011) for isotope values on calcite stalagmites, or on aragonite specimens that have been corrected to their calcite equivalent in the original publications, and the equilibrium fractionation equation of Grossman and Ku (1986) reformulated in Lachniet (2015) for aragonite samples to ensure consistency across records.

Based on the limited number of records available at the LGM, speleothem age uncertainties have only a limited impact on mean isotopic values, propagation of such uncertainties as well as any model uncertainties would substantially improve the robustness of data-model comparisons.

Based on our analyses, we therefore recommend that model evaluation using speleothem records should:

1. Filter speleothem records with respect to their mineralogy and use the appropriate equilibrium fractionation factor: Tremaine et al. (2011) for converting isotopic data from either calcite or aragonite-corrected-to-calcite samples to their drip water equivalent; and Grossman and Ku (1986) as reformulated by Lachniet (2015) for converting isotopic data from aragonite samples;
2. use the interval between 1850 and 1990 as the reference period for speleothem isotope records;
3. use speleothem isotopic data averaged for the intervals 6,000 ±500 yrs (21,000 ±1,000 yrs) for comparability with other MH (LGM) palaeoclimate benchmark datasets;
4. use speleothem isotopic data averaged for the interval 6,000 ±200 yrs or 21,000 ±500 yrs for best approximation of *midHolocene* and *lgm* experiments;

5. use absolute values only to assess data-model first order spatial patterns;
6. focus on multi-decadal to millennial timescales if using transient simulations for data-model comparisons.

5. Conclusions

Speleothem records show the same first-order spatial patterns as available in the Global Network of Isotopes in Precipitation (GNIP) data, and, therefore, are a good reflection of the $\delta^{18}O$ patterns in modern precipitation. This observation then suggests that stalagmites are a rich source of information for model evaluation. However, the inter-annual variability in the modern speleothem records is considerably reduced compared to the simulations, which in turn show less inter-annual variability than the GNIP observations. The low variability shown by the SISAL records – most likely from the low-pass filter effectively applied to the speleothem record by the karst system – precludes the use of this database for global studies focused on time scales shorter than quasi-decadal on a global basis.

Using the traditional anomaly approach to data-model comparisons, consistency between the sign of observed and simulated changes in both the MH and the LGM exists. However, the amplitude of modelled $\delta^{18}O$ changes is lower than the amplitude observed in the speleothem records. Thus, these kinds of comparisons should only focus on the large-scale spatial patterns that are significant, robust and climatologically interpretable. Based on the available SISAL data, the use of smaller time windows than the conventional definitions for each time slice does not have a strong impact on the mean values and could be used to reduce the uncertainties associated with the palaeodata. However, this would preclude comparisons with existing benchmark datasets that use the conventional windows for the MH and LGM time slices.

Only a limited number of speleothem records are continuous over long periods of time and the need to convert these to anomalies with respect to modern is a drawback. The limited number of records covering the LGM make the comparisons for this period particularly challenging. Nevertheless, continued expansion of SISAL database will increase its usefulness for model evaluation in future. Furthermore, we have shown that alternative approaches using absolute values could help examine spatial trends and diagnose systematic offsets.

Difficulties in constraining structural error on the model side and local controls on the observations complicate the derivation of comprehensive estimates of the true uncertainties of both simulations and observations. Site-specific controls can affect the $\delta^{18}O$ record captured in speleothems, but we have not screened for regionally anomalous records that could be influencing the results in our analyses. Our initial analyses suggest age uncertainty contributes little to the estimates for the LGM speleothem isotopic values. However, it is still important to propagate dating uncertainties for data-model comparison. Despite these challenges, SISAL appears to be an extremely useful tool for describing past patterns of variability, highlighting its potential for evaluating CMIP6-PMIP4 experiments.

6. Data availability

The version of the SISAL database used in this study is available in the University of Reading Research Data Archive (http://dx.doi.org/10.17864/1947.189). This dataset is cited in this manuscript as Atsawawaranunt et al., 2019.

7. Team list

SISAL working group members who coordinated data gathering for the SISAL database (listed in alphabetical order): Syed Masood Ahmad (Department of Geography, Faculty of Natural Sciences, Jamia Millia Islamia, New Delhi 110025, India), Yassine Ait Brahim (Institute of Global Environmental Change, Xi'an Jiaotong University, Xi'an, Shaanxi, China), Sahar Amirnezhad Mozhdehi (School of Earth Sciences, University College Dublin, Belfield. Dublin 4, Ireland), Monica Arienzo (Division of Hydrologic Sciences, Desert Research Institute, 2215 Raggio Parkway, 89512 Reno, NV, USA), Kamolphat Atsawawaranunt (School of Archaeology, Geography & Environmental Sciences, Reading University,

Clim. Past Discuss., https://doi.org/10.5194/cp-2019-25
Manuscript under review for journal Clim. Past
Discussion started: 4 March 2019

Climate of the Past Discussions

Whiteknights, Reading, RG6 6AH, UK), Andy Baker (School of Biological, Earth and Environmental Sciences, University of New South Wales, Kensington 2052, Australia), Kerstin Braun (Institute of Human Origins, Arizona State University, PO Box 874101, 85287 Tempe, Arizona, USA), Sebastian Breitenbach (Sediment & Isotope Geology, Institute of Geology, Mineralogy & Geophysics, Ruhr-Universität Bochum, Universitätsstr. 150, IA E5-179, 44801 Bochum, Germany), Yuval Burstyn (Geological Survey of Israel, 32 Yesha'yahu Leibowitz, 9371234, Jerusalem, Israel; Institute of Earth Sciences, Hebrew University of Jerusalem, Edmond J. Safra campus, Givat Ram, 91904 Jerusalem, Israel), Sakonvan Chawchai (MESA Research unit, Department of Geology, Faculty of Sciences, Chulalongkorn University, 254 Phayathai Rd, Pathum Wan, 10330 Bangkok, Thailand), Andrea Columbu (Department of Biological, Geological and Environmental Sciences, Via Zamboni 67, 40126, Bologna, Italy), Michael Deininger (Institute of Geosciences, Johannes Gutenberg University Mainz, Johann-Joachim-Becher-Weg 21, 55128 Mainz, Germany), Attila Demény (Institute for Geological and Geochemical Research, Research Centre for Astronomy and Earth Sciences, Hungarian Academy of Sciences, Budaörsi út 45, H-1112 Budapest, Hungary), Bronwyn Dixon (School of Archaeology, Geography & Environmental Sciences, Reading University, Whiteknights, Reading, RG6 6AH, UK and School of Geography, University of Melbourne, Melbourne, 3010, Australia), István Gábor Hatvani (Institute for Geological and Geochemical Research, Research Centre for Astronomy and Earth Sciences, Hungarian), Jun Hu (Department of Earth Sciences, University of Southern California, 3651 Trousdale Parkway, 90089 Los Angeles, California, USA), Nikita Kaushal (Department of Earth Sciences, University of Oxford, South Parks Road, Oxford, OX1 3AN, UK), Zoltán Kern (Institute for Geological and Geochemical Research, Research Centre for Astronomy and Earth Sciences, Hungarian Academy of Sciences, Budaörsi út 45, H-1112 Budapest, Hungary), Inga Labuhn (Institute of Geography, University of Bremen, Celsiusstr. 2, 28359 Bremen, Germany), Matthew S. Lachniet (Dept. of Geoscience, University of Nevada Las Vegas, Box 4022, 89154 Las Vegas, NV, USA), Franziska A. Lechleitner (Department of Earth Sciences, University of Oxford, South Parks Road, OX1 3AN Oxford, UK), Andrew Lorrey (National Institute of Water & Atmospheric Research, Climate Atmosphere and

Clim. Past Discuss., https://doi.org/10.5194/cp-2019-25
Manuscript under review for journal Clim. Past
Discussion started: 4 March 2019

Climate of the Past
Discussions

Hazards Centre, 41 Market Place, Viaduct Precinct, Auckland, New Zealand), Monika Markowska (University of Tübingen, Hölderlinstr. 12, 72074 Tübingen, Germany), Carole Nehme (IDEES UMR 6266 CNRS, Geography department, University of Rouen Normandie, Mont Saint Aignan, France), Valdir F. Novello (Instituto de Geociências, Universidade de São Paulo, São Paulo, Brazil), Jessica Oster (Department of Earth and Environmental Sciences, Vanderbilt University, Nashville, TN, 37206, USA), Carlos Pérez-Mejías (Department of Geoenvironmental Processes and Global Change, Pyrenean Institute of Ecology (IPE-CSIC), Avda. Montañana 1005, 50059 Zaragoza, Spain), Robyn Pickering (Department of Geological Sciences, University of Cape Town, University Avenue, Upper Campus, Room 208, 7701 Rondebosch, Cape Town, South Africa), Natasha Sekhon (Department of Geological Sciences, Jackson School of Geosciences, University of Texas, Austin, TX, 78712, USA), Xianfeng Wang (Earth Observatory of Singapore, Nanyang Technological University, Singapore 636798), Sophie Warken (Institute of Environmental Physics, Ruprecht-Karls-Universität Heidelberg, Im Neuenheimer Feld 229, 69120 Heidelberg, Germany.

SISAL working members who submitted data to the SISAL database (listed in alphabetical order): Tim Atkinson (Departments of Earth Sciences & Geography, University College London, WC1E 6BT, United Kingdom), Avner Ayalon (Geological Survey of Israel, 32 Yesha'yahu Leibowitz, Jerusalem, 9371234), James Baldini (Department of Earth Sciences, Durham University, DH1 3LE, United Kingdom), Miryam Bar-Matthews (Geological Survey of Israel, 32 Yesha'yahu Leibowitz, Jerusalem, 9371234), Juan Pablo Bernal (Centro de Geociencias, Universidad Nacional Autónoma de México, Campus UNAM Juriquilla, Querétaro 76230, Querétaro, Mexico), Ronny Boch (Graz University of Technology. Institute of Applied Geosciences. Rechbauerstrasse 12, 8010 Graz, Austria), Andrea Borsato (School of Environmental and Life Science, University of Newcastle, 2308 NSW, Australia), Meighan Boyd (Department of Earth Sciences, Royal Holloway University of London, Egham, Surrey TW20 0EX, UK), Chris Brierley (Department of Geography, University College London, WC1E 6BT, United Kingdom), Yanjun Cai (State Key Lab of Loess and Quaternary Geology, Institute of Earth Environment, Chinese Academy of Sciences, Xi'an 710061, China), Stacy Carolin (Institute of Geology, University of Innsbruck,

Clim. Past Discuss., https://doi.org/10.5194/cp-2019-25
Manuscript under review for journal Clim. Past
Discussion started: 4 March 2019

Innrain 52, 6020 Innsbruck, Austria), Hai Cheng (Institute of Global Environmental Change, Xi'an Jiaotong University, China), Silviu Constantin (Emil Racovita Institute of Speleology, str. Frumoasa 31, Bucharest, Romania), Isabelle Couchoud (EDYTEM, UMR 5204 CNRS, Université Savoie Mont Blanc, Université Grenoble Alpes, 73370 Le Bourget du Lac, France), Francisco Cruz (Instituto de Geociências, Universidade de São Paulo, São Paulo, Brazil), Rhawn Denniston (Department of Geology, Cornell College, Mount Vernon, IA, 52314, USA), Virgil Drăguşin (Emil Racovita Institute of Speleology, str. Frumoasa 31, Bucharest, Romania), Wuhui Duan (Key Laboratory of Cenozoic Geology and Environment, Institute of Geology and Geophysics, Chinese Academy of Sciences, Beijing, China, 100029, Vasile Ersek (Department of Geography and Environmental Sciences, Northumbria University, Newcastle upon Tyne, UK), Martin Finné (Department of Archaeology and Ancient History, Uppsala University, Sweden), Dominik Fleitmann (Department of Archaeology. School of Archaeology, Geography and Environmental Science. Whiteknights. University of Reading RG6 6AB, UK), Jens Fohlmeister (Institute for Earth and Environmental Sciences, University of Potsdam, Karl-Liebknecht-Str. 24-25, 14476 Potsdam, Germany), Amy Frappier (Department of Geosciences, Skidmore College, Saratoga Springs, NY 12866 US), Dominique Genty (Laboratoire des Science du Climat et de l'Environment, CNRS, L'Orme des Merisiers, 91191 Gif-sure-Yvette Cedex, France), Steffen Holzkämper (Department of Physical Geography. Stockholm University. 106 91 Stockholm, Sweden), Philip Hopley (Department of Earth and Planetary Sciences, Birkbeck, University of London, Malet St, London, WC1E 7HX), Vanessa Johnston (Karst Research Institute, Research Centre of the Slovenian Academy of Sciences and Arts, Titov trg 2, SI-6230, Postojna, Slovenia), Gayatri Kathayat (Institute of Global Environmental Change, Xi'an Jiaotong University, China), Duncan Keenan-Jones (School of Historical and Philosophical Inquiry, University of Queensland, St Lucia QLD 4072, Australia), Gabriella Koltai (Institute of Geology, University of Innsbruck, Innrain 52, 6020 Innsbruck, Austria), Ting-Yong Li (Chongqing Key Laboratory of Karst Environment, School of Geographical Sciences, Southwest University, Chongqing 400715, China, and Field Scientific Observation & Research Base of Karst Eco-environments at Nanchuan in Chongqing, Ministry of Nature Resources of China, Chongqing 408435,

Clim. Past Discuss., https://doi.org/10.5194/cp-2019-25
Manuscript under review for journal Clim. Past
Discussion started: 4 March 2019

China), Marc Luetscher (Swiss Institute for Speleology and Karst Studies (SISKA), Rue de la Serre 68, CH-2301 La Chaux-de-Fonds, Switzerland), Dave Mattey (Department of Earth Sciences, Royal Holloway University of London, Egham, Surrey, TW20 0EX, UK), Ana Moreno (Dpto. de Procesos Geoambientales y Cambio Global. Instituto Pirenaico de Ecología-CSIC. Zaragoza, Spain), Gina Moseley (Institute of Geology, University of Innsbruck, Innrain 52, 6020 Innsbruck, Austria), David Psomiadis (Imprint Analytics GmbH, Werner von Siemens Str. 1, A7343 Neutal, Austria), Jiaoyang Ruan (Guangdong Provincial Key Lab of Geodynamics and Geohazards, School of Earth Sciences and Engineering, Sun Yat-sen University, Guangzhou 510275, China), Denis Scholz (Institute for Geosciences, University of Mainz, Johann-Joachim-Becher-Weg 21, 55128 Mainz, Germany), Lijuan Sha (Institute of Global Environmental Change, Xi'an Jiaotong University, Xi'an, Shaanxi, China), James Baucher 5, Sofia 1164, Bulgaria), Andrew Christopher Smith (NERC Isotope Geoscience Facility, British Geological Survey, Nottingham, UK), Nicolás Strikis (Departamento de Geoquímica, Universidade Federal Fluminense, Niterói, Brazil), Pauline Treble (ANSTO, Lucas Heights NSW, Australia), Ezgi Ünal-İmer (Department of Geological Engineering, Middle East Technical University, Ankara, Turkey), Anton Vaks (Geological Survey of Israel, 32 Yesha'yahu Leibowitz, Jerusalem, 9371234), Stef Vansteenberge (Analytical, Environmental & Geo-Chemistry, Department of Chemistry, Vrije Universiteit Brussel, Belgium), Ny Riavo G. Voarintsoa (Institute of Earth Sciences, The Hebrew University in Jerusalem, Israel), Corinne Wong (Environmental Science Institute, The University of Texas at Austin, 2275 Speedway, Austin TX 78712, USA), Barbara Wortham (Department of Earth and Planetary Science, University of California, Davis, USA), Jennifer Wurtzel (Research School of Earth Sciences, Australian National University, Canberra, ACT, Australia / ARC Centre of Excellence for Climate System Science, Australian National University, Canberra, ACT, Australia), Haiwei Zhang (Institute of Global Environmental Change, Xi'an Jiaotong University, China).

8. Author contribution

LCB is the coordinator of the SISAL working group. LCB and SPH designed the study. LCB and SPH wrote the first draft of the manuscript with contributions from MW, NS, KR, CVP. LCB did the analyses and created Figs. 1, 2-5, 7, 8 and Supplementary Figs. 1-5. MW provided the ECHAM5-wiso model simulations and helped on its analyses. NS did the analyses on speleothem growth over time and created Fig. 2. KR did the analysis on the LGM uncertainties and created Fig. 6. CVP did the multivariate linear analyses (Supplementary material). All authors contributed to the last version of this manuscript. The authors listed in the "SISAL working group" team contributed to this study coordinating data gathering, database construction or with speleothem data submitted to the SISAL database. SB created the COPRA age-depth models used in this study. TA and DG contributed original unpublished data to the SISAL database. JB, AB, ZK, MA, MSL, VJ, BW and SB helped edit the manuscript.

9. Competing interests

The authors declare that they have no conflict of interest.

10. Acknowledgements

SISAL (Speleothem Isotopes Synthesis and Analysis) is a working group of the Past Global Changes (PAGES) programme. We thank PAGES for their support for this activity. Additional financial support for SISAL activities has been provided by the European Geosciences Union (EGU TE Winter call, grant number W2017/413), Irish Centre for Research in Applied Geosciences (iCRAG), European Association of Geochemistry (Early Career Ambassadors program 2017), Quaternary Research Association UK, Navarino Environmental Observatory, Stockholm University, Savillex, John Cantle, University of Reading (UK), University College Dublin (Ireland; Seed Funding award, grant number SF1428), and University Ibn Zohr (Morocco). L.C.B. and S.P.H. acknowledge support from the ERC-funded project GC2.0 (Global Change 2.0: Unlocking the past for a clearer future, grant number 694481). S.P.H. also acknowledges support from the JPI-Belmont project "PAleao-Constraints on Monsoon Evolution and

Dynamics (PACMEDY)" through the UK Natural Environmental Research Council (NERC). L.C.B. also acknowledges support from the Geological Survey Ireland (Short Call 2017; grant number 2017-SC-056) and the Royal Irish Academy's Charlemont Scholar award 2018. C.V.P. acknowledges funding from the Portuguese Science Foundation (FCT) through the CIMA research center project (UID/MAR/00350/2013). K.R. was supported by Deutsche Forschungsgemeinschaft (DFG) grant no. RE3994/2-1. We thank the World Karst Aquifer Mapping project (WOKAM) team for providing us with the karst map presented in Fig. 1a. The authors would like to thank the following data contributors: Dominique Blamart, Jean Riotte, Russell Drysdale, Petra Bajo and Frank McDermott.

11. References

Atkinson, T. C.: Carbon dioxide in the atmosphere of the unsaturated zone: An important control of groundwater hardness in limestones, Journal of Hydrology, 35, 111-123, https://doi.org/10.1016/0022-1694(77)90080-4, 1977.

Atsawawaranunt, K., Comas-Bru, L., Amirnezhad Mozhdehi, S., Deininger, M., Harrison, S. P., Baker, A., Boyd, M., Kaushal, N., Ahmad, S. M., Ait Brahim, Y., Arienzo, M., Bajo, P., Braun, K., Burstyn, Y., Chawchai, S., Duan, W., Hatvani, I. G., Hu, J., Kern, Z., Labuhn, I., Lachniet, M., Lechleitner, F. A., Lorrey, A., Pérez-Mejías, C., Pickering, R., Scroxton, N., and Members, S. W. G.: The SISAL database: a global resource to document oxygen and carbon isotope records from speleothems, Earth Syst. Sci. Data, 10, 1687-1713, https://doi.org/10.5194/essd-10-1687-2018, 2018a.

Atsawawaranunt, K., Harrison, S. and Comas-Bru, L.: SISAL (Speleothem Isotopes Synthesis and AnaLysis Working Group) database Version 1.0. University of Reading. Dataset. : https://doi.org/10.17864/1947.147, 2018b.

Atsawawaranunt, K., Harrison, S. and Comas-Bru, L.: SISAL (Speleothem Isotopes Synthesis and AnaLysis Working Group) database Version 1b. University of Reading. Dataset. : https://doi.org/10.17864/1947.189, 2019.

Ayliffe, L. K., Marianelli, P. C., Moriarty, K. C., Wells, R. T., McCulloch, M. T., Mortimer, G. E., and Hellstrom, J. C.: 500 ka precipitation record from southeastern Australia: Evidence for interglacial relative aridity, Geology, 26, 147-150, https://doi.org/10.1130/0091-7613(1998)026<0147:kprfsa>2.3.co;2, 1998.

Badertscher, S., Fleitmann, D., Cheng, H., Edwards, R. L., Gokturk, O. M., Zumbuhl, A., Leuenberger, M., and Tuysuz, O.: Pleistocene water intrusions from the Mediterranean and Caspian seas into the Black Sea, Nature Geoscience, 4, 236-239, https://doi.org/10.1038/ngeo1106, 2011.

Clim. Past Discuss., https://doi.org/10.5194/cp-2019-25
Manuscript under review for journal Clim. Past
Discussion started: 4 March 2019

Climate of the Past
Discussions
Open Access

Baker, A., Bradley, C., and Phipps, S. J.: Hydrological modeling of stalagmite δ18O response to glacial-interglacial transitions, Geophysical Research Letters, 40, 3207-3212, https://doi.org/10.1002/grl.50555, 2013.

Bar-Matthews, M., Ayalon, A., Gilmour, M., Matthews, A., and Hawkesworth, C. J.: Sea-land oxygen isotopic relationships from planktonic foraminifera and speleothems in the Eastern Mediterranean region and their implication for paleorainfall during interglacial intervals, Geochimica Et Cosmochimica Acta, 67, 3181-3199, https://doi.org/10.1016/s0016-7037(02)01031-1, 2003.

Bartlein, P. J., Harrison, S. P., Brewer, S., Connor, S., Davis, B. A. S., Gajewski, K., Guiot, J., Harrison-Prentice, T. I., Henderson, A., Peyron, O., Prentice, I. C., Scholze, M., Seppä, H., Shuman, B., Sugita, S., Thompson, R. S., Viau, A. E., Williams, J., and Wu, H.: Pollen-based continental climate reconstructions at 6 and 21 ka: a global synthesis, Climate Dynamics, 37, 775-802, https://doi.org/10.1007/s00382-010-0904-1, 2011.

Boch, R., Cheng, H., Spotl, C., Edwards, R. L., Wang, X., and Hauselmann, P.: NALPS: a precisely dated European climate record 120-60 ka, Climate of the Past, 7, 1247-1259, https://doi.org/10.5194/cp-7-1247-2011, 2011.

Bowen, G. J., and Revenaugh, J.: Interpolating the isotopic composition of modern meteoric precipitation, Water Resources Research, 39, https://doi.org/10.1029/2003WR002086, 2003.

Gridded maps of the isotopic composition of meteoric waters., access: October 2018, 2018.

Braconnot, P., Harrison, S. P., Kageyama, M., Bartlein, P. J., Masson-Delmotte, V., Abe-Ouchi, A., Otto-Bliesner, B., and Zhao, Y.: Evaluation of climate models using palaeoclimatic data, Nature Climate Change, 2, 417, https://doi.org/10.1038/nclimate1456, 2012.

Breitenbach, S. F. M., Rehfeld, K., Goswami, B., Baldini, J. U. L., Ridley, H. E., Kennett, D. J., Prufer, K. M., Aquino, V. V., Asmerom, Y., Polyak, V. J., Cheng, H., Kurths, J., and Marwan, N.: COnstructing Proxy Records from Age models (COPRA), Clim. Past, 8, 1765-1779, https://doi.org/10.5194/cp-8-1765-2012, 2012.

Breitenbach, S. F. M., Lechleitner, F. A., Meyer, H., Diengdoh, G., Mattey, D., and Marwan, N.: Cave ventilation and rainfall signals in dripwater in a monsoonal setting – a monitoring study from NE India, Chemical Geology, 402, 111-124, https://doi.org/10.1016/J.CHEMGEO.2015.03.011, 2015.

Bustamante, M. G., Cruz, F. W., Vuille, M., Apaestegui, J., Strikis, N., Panizo, G., Novello, F. V., Deininger, M., Sifeddine, A., Cheng, H., Moquet, J. S., Guyot, J. L., Santos, R. V., Segura, H., and Edwards, R. L.: Holocene changes in monsoon precipitation in the Andes of NE Peru based on delta O-18 speleothem records, Quaternary Science Reviews, 146, 274-287, https://doi.org/10.1016/j.quascirev.2016.05.023, 2016.

Butzin, M., Werner, M., Masson-Delmotte, V., Risi, C., Frankenberg, C., Gribanov, K., Jouzel, J., and Zakharov, V. I.: Variations of oxygen-18 in West Siberian precipitation during the last 50 years, Atmos. Chem. Phys., 14, 5853-5869, https://doi.org/10.5194/acp-14-5853-2014, 2014.

Caley, T., and Roche, D. M.: delta O-18 water isotope in the iLOVECLIM model (version 1.0) - Part 3: A palaeo-perspective based on present-day data-model comparison for oxygen stable isotopes in carbonates, Geoscientific Model Development, 6, 1505-1516, https://doi.org/10.5194/gmd-6-1505-2013, 2013.

Caley, T., Roche, D. M., Waelbroeck, C., and Michel, E.: Oxygen stable isotopes during the Last Glacial Maximum climate: perspectives from data-model (iLOVECLIM) comparison, Climate of the Past, 10, 1939-1955, https://doi.org/10.5194/cp-10-1939-2014, 2014.

Chen, Z., Auler, A. S., Bakalowicz, M., Drew, D., Griger, F., Hartmann, J., Jiang, G., Moosdorf, N., Richts, A., Stevanovic, Z., Veni, G., and Goldscheider, N.: The World Karst Aquifer Mapping project: concept, mapping procedure and map of Europe, Hydrogeology Journal, 25, 771-785, https://doi.org/10.1007/s10040-016-1519-3, 2017.

Cheng, H., Fleitmann, D., Edwards, R. L., Wang, X., Cruz, F. W., Auler, A. S., Mangini, A., Wang, Y., Kong, X., Burns, S. J., and Matter, A.: Timing and structure of the 8.2 kyr B.P. event inferred from δ18O records of stalagmites from China, Oman, and Brazil, Geology, 37, 1007-1010, https://doi.org/10.1130/G30126A.1, 2009.

Cheng, H., Sinha, A., Cruz, F. W., Wang, X., Edwards, R. L., d'Horta, F. M., Ribas, C. C., Vuille, M., Stott, L. D., and Auler, A. S.: Climate change patterns in Amazonia and biodiversity, Nature Communications, 4, 1411-1411, https://doi.org/10.1038/ncomms2415, 2013.

Christensen, J. H., Kanikicharla, K. K., Marshall, G., and Turner, J.: Climate phenomena and their relevance for future regional climate change, in: Climate Change 2013 – The Physical Science Basis: Working Group I Contribution to the Fifth Assessment Report of the Intergovernmental Panel on Climate Change, edited by: Change, I. P. o. C., Cambridge University Press, Cambridge, 1217-1308, 2013.

Collins, M., Knutti, R., Arblaster, J., Dufresne, J.-L., Fichefet, T., Friedlingstein, P., Gao, X., Gutowski, W., Johns, T., and Krinner, G.: Long-term climate change: projections, commitments and irreversibility, in: Climate Change 2013 – The Physical Science Basis: Working Group I Contribution to the Fifth Assessment Report of the Intergovernmental Panel on Climate Change, edited by: Change, I. P. o. C., Cambridge University Press, Cambridge, 1029-1136, 2013.

Collins, W. D., Bitz, C. M., Blackmon, M. L., Bonan, G. B., Bretherton, C. S., Carton, J. A., Chang, P., Doney, S. C., Hack, J. J., Henderson, T. B., Kiehl, J. T., Large, W. G., McKenna, D. S., Santer, B. D., and Smith, R. D.: The Community Climate System Model Version 3 (CCSM3), Journal of Climate, 19, 2122-2143, https://doi.org/10.1175/jcli3761.1, 2006.

Columbu, A., Sauro, F., Lundberg, J., Drysdale, R., and De Waele, J.: Palaeoenvironmental changes recorded by speleothems of the southern Alps (Piani Eterni, Belluno, Italy) during four interglacial to glacial climate transitions, Quaternary Science Reviews, 197, 319-335, https://doi.org/10.1016/J.QUASCIREV.2018.08.006, 2018.

Comas-Bru, L., and Harrison, S. P.: SISAL: Bringing added value to speleothem research, Quaternary, 2(1), https://doi.org/10.3390/quat2010007, 2019.

Clim. Past Discuss., https://doi.org/10.5194/cp-2019-25
Manuscript under review for journal Clim. Past
Discussion started: 4 March 2019

Climate of the Past Discussions
Open Access

Constantin, S., Bojar, A. V., Lauritzen, S. E., and Lundberg, J.: Holocene and Late Pleistocene climate in the sub-Mediterranean continental environment: A speleothem record from Poleva Cave (Southern Carpathians, Romania), Palaeogeography Palaeoclimatology Palaeoecology, 243, 322-338, https://doi.org/10.1016/j.palaeo.2006.08.001, 2007.

Coplen, T. B., Kendall, C., and Hopple, J.: Comparison of stable isotope reference samples, Nature, 302, 236-238, https://doi.org/10.1038/302236a0, 1983.

Cosford, J., Qing, H., Eglington, B., Mattey, D., Yuan, D., Zhang, M., and Cheng, H.: East Asian monsoon variability since the Mid-Holocene recorded in a high-resolution, absolute-dated aragonite speleothem from eastern China, Earth and Planetary Science Letters, 275, 296-307, https://doi.org/10.1016/J.EPSL.2008.08.018, 2008a.

Cosford, J., Qing, H., Yuan, D., Zhang, M., Holmden, C., Patterson, W., and Hai, C.: Millennial-scale variability in the Asian monsoon: Evidence from oxygen isotope records from stalagmites in southeastern China, Palaeogeography, Palaeoclimatology, Palaeoecology, 266, 3-12, https://doi.org/10.1016/J.PALAEO.2008.03.029, 2008b.

Cruz, F. W., Burns, S. J., Karmann, I., Sharp, W. D., Vuille, M., Cardoso, A. O., Ferrari, J. A., Dias, P. L. S., and Viana, O.: Insolation-driven changes in atmospheric circulation over the past 116,000 years in subtropical Brazil, Nature, 434, 63-66, https://doi.org/10.1038/nature03365, 2005.

Daëron, M., Drysdale, R. N., Peral, M., Huyghe, D., Blamart, D., Coplen, T. B., Lartaud, F., and Zanchetta, G.: Most Earth-surface calcites precipitate out of isotopic equilibrium, Nature Communications, 10, 429, https://doi.org/10.1038/s41467-019-08336-5, 2019.

Dansgaard, W.: Stable isotopes in precipitation, Tellus, 16, 436-468, 1964.

Denniston, R. F., González, L. A., Asmerom, Y., Baker, R. G., Reagan, M. K., and Bettis, E. A.: Evidence for increased cool season moisture during the middle Holocene, Geology, 27, 815-815, https://doi.org/10.1130/0091-7613(1999)027<0815:EFICSM>2.3.CO;2, 1999.

Denniston, R. F., Asmerom, Y., Polyak, V., Dorale, J. A., Carpenter, S. J., Trodick, C., Hoye, B., and Gonzalez, L. A.: Synchronous millennial-scale climatic changes in the Great Basin and the North Atlantic during the last interglacial, Geology, 35, 619-622, https://doi.org/10.1130/g23445a.1, 2007a.

Denniston, R. F., DuPree, M., Dorale, J. A., Asmerom, Y., Polyak, V. J., and Carpenter, S. J.: Episodes of late Holocene aridity recorded by stalagmites from Devil's icebox Cave, Central Missouri, USA, Quaternary Research, 68, 45-52, https://doi.org/10.1016/j.yqres.2007.04.001, 2007b.

Denniston, R. F., Wyrwoll, K. H., Polyak, V. J., Brown, J. R., Asmerom, Y., Wanamaker, A. D., LaPointe, Z., Ellerbroek, R., Barthelmes, M., Cleary, D., Cugley, J., Woods, D., and Humphreys, W. F.: A Stalagmite record of Holocene Indonesian-Australian summer monsoon variability from the Australian tropics, Quaternary Science Reviews, 78, 155-168, https://doi.org/10.1016/j.quascirev.2013.08.004, 2013.

Dykoski, C. A., Edwards, R. L., Cheng, H., Yuan, D., Cai, Y., Zhang, M., Lin, Y., Qing, J., An, Z., and Revenaugh, J.: A high-resolution, absolute-dated Holocene and deglacial Asian monsoon record from Dongge Cave, China, Earth and Planetary Science Letters, 233, 71-86, https://doi.org/10.1016/J.EPSL.2005.01.036, 2005.

Fairchild, I., and Baker, A.: Speleothem Science: From Process to Past Environments, Blackwell Quaternary Geoscience Series, edited by: Bradley, R., Wiley-Blackwell, United Kingdom, 432 pp., 2012.

Fensterer, C., Scholz, D., Hoffmann, D., Mangini, A., and Pajón, J. M.: ²³⁰ Th/U-dating of a late Holocene low uranium speleothem from Cuba, IOP Conference Series: Earth and Environmental Science, 9, 012015-012015, https://doi.org/10.1088/1755-1315/9/1/012015, 2010.

Fensterer, C., Scholz, D., Hoffmann, D., Spotl, C., Pajon, J. M., and Mangini, A.: Cuban stalagmite suggests relationship between Caribbean precipitation and the Atlantic Multidecadal Oscillation during the past 1.3 ka, Holocene, 22, 1405-1412, https://doi.org/10.1177/0959683612449759, 2012.

Field, C. B.: Climate change 2014–Impacts, adaptation and vulnerability: Regional aspects, Cambridge University Press, 2014.

Fischer, M. J., and Treble, P. C.: Calibrating climate-delta O-18 regression models for the interpretation of high-resolution speleothem delta O-18 time series, Journal of Geophysical Research-Atmospheres, 113, https://doi.org/10.1029/2007jd009694, 2008.

Fleitmann, D., Burns, S. J., Neff, U., Mangini, A., and Matter, A.: Changing moisture sources over the last 330,000 years in Northern Oman from fluid-inclusion evidence in speleothems, Quaternary Research, 60, 223-232, https://doi.org/10.1016/s0033-5894(03)00086-3, 2003.

Fleitmann, D., Cheng, H., Badertscher, S., Edwards, R. L., Mudelsee, M., Gokturk, O. M., Fankhauser, A., Pickering, R., Raible, C. C., Matter, A., Kramers, J., and Tuysuz, O.: Timing and climatic impact of Greenland interstadials recorded in stalagmites from northern Turkey, Geophysical Research Letters, 36, https://doi.org/10.1029/2009gl040050, 2009.

Gascoyne, M., Schwarcz, H. P., Ford, D. C., and Thode, H. G.: Uranium-series ages of speleothem from northwest England: correlation with Quaternary climate, Philosophical Transactions of the Royal Society of London. B, Biological Sciences, 301, 143-164, https://doi.org/10.1098/rstb.1983.0024, 1983.

Göktürk, O. M., Fleitmann, D., Badertscher, S., Cheng, H., Edwards, R. L., Leuenberger, M., Fankhauser, A., Tüysüz, O., and Kramers, J.: Climate on the southern Black Sea coast during the Holocene: implications from the Sofular Cave record, Quaternary Science Reviews, 30, 2433-2445, https://doi.org/10.1016/J.QUASCIREV.2011.05.007, 2011.

Grossman, E. L., and Ku, T.-L.: Oxygen and carbon isotope fractionation in biogenic aragonite: Temperature effects, Chemical Geology: Isotope Geoscience section, 59, 59-74, https://doi.org/10.1016/0168-9622(86)90057-6, 1986.

Hagemann, S., Arpe, K., and Roeckner, E.: Evaluation of the Hydrological Cycle in the ECHAM5 Model, Journal of Climate, 19, 3810-3827, https://doi.org/10.1175/JCLI3831.1, 2006.

Harris, I., Jones, P. D., Osborn, T. J., and Lister, D. H.: Updated high-resolution grids of monthly climatic observations – the CRU TS3.10 Dataset, International Journal of Climatology, 34, 623-642, https://doi.org/10.1002/joc.3711, retrieved from https://crudata.uea.ac.uk/cru/data/hrg/cru_ts_4.01/ on November 2018,, 2014.

Harrison, S. P., Bartlein, P. J., Brewer, S., Prentice, I. C., Boyd, M., Hessler, I., Holmgren, K., Izumi, K., and Willis, K.: Climate model benchmarking with glacial and mid-Holocene climates, Climate Dynamics, 43, 671-688, https://doi.org/10.1007/s00382-013-1922-6, 2014.

Hartmann, A., Eiche, E., Neumann, T., Fohlmeister, J., Schroder-Ritzrau, A., Mangini, A., and Haryono, E.: Multi-proxy evidence for human-induced deforestation and cultivation from a late Holocene stalagmite from middle Java, Indonesia, Chemical Geology, 357, 8-17, https://doi.org/10.1016/j.chemgeo.2013.08.026, 2013.

Hessler, I., Harrison, S. P., Kucera, M., Waelbroeck, C., Chen, M. T., Anderson, C., de Vernal, A., Fréchette, B., Cloke-Hayes, A., Leduc, G., and Londeix, L.: Implication of methodological uncertainties for mid-Holocene sea surface temperature reconstructions, Clim. Past, 10, 2237-2252, https://doi.org/10.5194/cp-10-2237-2014, 2014.

Hoffmann, G., Werner, M., and Heimann, M.: Water isotope module of the ECHAM atmospheric general circulation model: A study on timescales from days to several years, Journal of Geophysical Research: Atmospheres, 103, 16871-16896, 1998.

Hoffmann, G., Jouzel, J., and Masson, V.: Stable water isotopes in atmospheric general circulation models, Hydrological Processes, 14, 1385-1406, https://doi.org/10.1002/1099-1085(20000615)14:8<1385::AID-HYP989>3.0.CO;2-1, 2000.

Hu, J., Emile-Geay, J., Nusbaumer, J., and Noone, D.: Impact of Convective Activity on Precipitation δ18O in Isotope-Enabled General Circulation Models, Journal of Geophysical Research: Atmospheres, 123, 13,595-513,610, https://doi.org/10.1029/2018JD029187, 2018.

IAEA/WMO: Global Network of Isotopes in Precipitation. The GNIP Database., 2017.

IAEA/WMO: Global Network of Isotopes in Precipitation. The GNIP Database., 2018.

Jasechko, S., Lechler, A., Pausata, F. S. R., Fawcett, P. J., Gleeson, T., Cendón, D. I., Galewsky, J., LeGrande, A. N., Risi, C., Sharp, Z. D., Welker, J. M., Werner, M., and Yoshimura, K.: Late-glacial to late-Holocene shifts in global precipitation δ¹⁸O, Clim. Past, 11, 1375-1393, https://doi.org/10.5194/cp-11-1375-2015, 2015.

Jo, K. N., Woo, K. S., Yi, S., Yang, D. Y., Lim, H. S., Wang, Y. J., Cheng, H., and Edwards, R. L.: Mid-latitude interhemispheric hydrologic seesaw over the past 550,000 years, Nature, 508, 378-+, https://doi.org/10.1038/nature13076, 2014.

Johnston, V. E., Borsato, A., Frisia, S., Spotl, C., Dublyansky, Y., Tochterle, P., Hellstrom, J. C., Bajo, P., Edwards, R. L., and Cheng, H.: Evidence of thermophilisation and elevationdependent warming during the Last Interglacial in the Italian Alps, Scientific Reports, 8, https://doi.org/10.1038/s41598-018-21027-3, 2018.

Joussaume, S., Sadourny, R., and Jouzel, J.: A general circulation model of water isotope cycles in the atmosphere, Nature, 311, 24-29, https://doi.org/10.1038/311024a0, 1984.

Jouzel, J., Hoffmann, G., Koster, R. D., and Masson, V.: Water isotopes in precipitation:: data/model comparison for present-day and past climates, Quaternary Science Reviews, 19, 363-379, https://doi.org/10.1016/S0277-3791(99)00069-4, 2000.

Kageyama, M., Albani, S., Braconnot, P., Harrison, S. P., Hopcroft, P. O., Ivanovic, R. F., Lambert, F., Marti, O., Peltier, W. R., Peterschmitt, J. Y., Roche, D. M., Tarasov, L., Zhang, X., Brady, E. C., Haywood, A. M., LeGrande, A. N., Lunt, D. J., Mahowald, N. M., Mikolajewicz, U., Nisancioglu, K. H., Otto-Bliesner, B. L., Renssen, H., Tomas, R. A., Zhang, Q., Abe-Ouchi, A., Bartlein, P. J., Cao, J., Li, Q., Lohmann, G., Ohgaito, R., Shi, X., Volodin, E., Yoshida, K., Zhang, X., and Zheng, W.: The PMIP4 contribution to CMIP6 – Part 4: Scientific objectives and experimental design of the PMIP4-CMIP6 Last Glacial Maximum experiments and PMIP4 sensitivity experiments, Geosci. Model Dev., 10, 4035-4055, https://doi.org/10.5194/gmd-10-4035-2017, 2017.

Kim, S.-T., and O'Neil, J. R.: Equilibrium and nonequilibrium oxygen isotope effects in synthetic carbonates, Geochimica et Cosmochimica Acta, 61, 3461-3475, https://doi.org/10.1016/S0016-7037(97)00169-5, 1997.

Kirtman, B., Power, S. B., Adedoyin, A. J., Boer, G. J., Bojariu, R., Camilloni, I., Doblas-Reyes, F., Fiore, A. M., Kimoto, M., and Meehl, G.: Near-term Climate Change: Projections and Predictability, in: Climate Change 2013 – The Physical Science Basis: Working Group I Contribution to the Fifth Assessment Report of the Intergovernmental Panel on Climate Change, edited by: Change, I. P. o. C., Cambridge University Press, Cambridge, 953-1020, 2013.

Lachniet, M. S.: Climatic and environmental controls on speleothem oxygen-isotope values, Quaternary Science Reviews, 28, 412-432, https://doi.org/10.1016/j.quascirev.2008.10.021, 2009.

Lachniet, M. S.: Are aragonite stalagmites reliable paleoclimate proxies? Tests for oxygen isotope time-series replication and equilibrium, GSA Bulletin, 127, 1521-1533, https://doi.org/10.1130/B31161.1, 2015.

Langebroek, P. M., Werner, M., and Lohmann, G.: Climate information imprinted in oxygen-isotopic composition of precipitation in Europe, Earth and Planetary Science Letters, 311, 144-154, https://doi.org/10.1016/j.epsl.2011.08.049, 2011.

Lauritzen, S. E., and Lundberg, J.: Calibration of the speleothem delta function: an absolute temperature record for the Holocene in northern Norway, Holocene, 9, 659-669, https://doi.org/10.1191/095968399667823929, 1999.

LeGrande, A. N., and Schmidt, G. A.: Ensemble, water isotope–enabled, coupled general circulation modeling insights into the 8.2 ka event, Paleoceanography, 23, https://doi.org/10.1029/2008PA001610, 2008.

LeGrande, A. N., and Schmidt, G. A.: Sources of Holocene variability of oxygen isotopes in paleoclimate archives, Climate of the Past, 5, 441-455, https://doi.org/10.5194/cp-5-441-2009, 2009.

Lundeen, Z., Brunelle, A., Burns, S. J., Polyak, V., and Asmerom, Y.: A speleothem record of Holocene paleoclimate from the northern Wasatch Mountains, southeast Idaho, USA, Quaternary International, 310, 83-95, https://doi.org/10.1016/J.QUAINT.2013.03.018, 2013.

Mangini, A., Blumbach, P., Verdes, P., Spotl, C., Scholz, D., Machel, H., and Mahon, S.: Combined records from a stalagmite from Barbados and from lake sediments in Haiti reveal variable seasonality in the Caribbean between 6.7 and 3 ka BP, Quaternary Science Reviews, 26, 1332-1343, https://doi.org/10.1016/j.quascirev.2007.01.011, 2007.

Marshall, D., Ghaleb, B., Countess, R., and Gabities, J.: Preliminary paleoclimate reconstruction based on a 12,500 year old speleothem from Vancouver Island, Canada: stable isotopes and U-Th disequilibrium dating, Quaternary Science Reviews, 28, 2507-2513, https://doi.org/10.1016/j.quascirev.2009.05.019, 2009.

McDermott, F.: Palaeo-climate reconstruction from stable isotope variations in speleothems: a review, Quaternary Science Reviews, 23, 901-918, https://doi.org/10.1016/j.quascirev.2003.06.021, 2004.

McDermott, F., Atkinson, T. C., Fairchild, I. J., Baldini, L. M., and Mattey, D. P.: A first evaluation of the spatial gradients in delta O-18 recorded by European Holocene speleothems, Global and Planetary Change, 79, 275-287, https://doi.org/10.1016/j.gloplacha.2011.01.005, 2011.

MARGO project members: Constraints on the magnitude and patterns of ocean cooling at the Last Glacial Maximum, Nature Geoscience, 2, 127, https://doi.org/10.1038/ngeo411, 2009.

Mickler, P. J., Banner, J. L., Stern, L., Asmerom, Y., Edwards, R. L., and Ito, E.: Stable isotope variations in modern tropical speleothems: Evaluating equilibrium vs. kinetic isotope effects, Geochimica et Cosmochimica Acta, 68, 4381-4393, https://doi.org/10.1016/J.GCA.2004.02.012, 2004.

Mickler, P. J., Stern, L. A., and Banner, J. L.: Large kinetic isotope effects in modern speleothems, Geological Society of America Bulletin, 118, 65-81, https://doi.org/10.1130/B25698.1, 2006.

Moore, G. W., and Sullivan, N.: Spelology Caves and the Cave Environment, 3rd Edition ed., Cave Books, St. Louis, 1997.

Myers, C. G., Oster, J. L., Sharp, W. D., Bennartz, R., Kelley, N. P., Covey, A. K., and Breitenbach, S. F. M.: Northeast Indian stalagmite records Pacific decadal climate change: Implications for moisture transport and drought in India, Geophysical Research Letters, 42, 4124-4132, https://doi.org/10.1002/2015GL063826, 2015.

Clim. Past Discuss., https://doi.org/10.5194/cp-2019-25
Manuscript under review for journal Clim. Past
Discussion started: 4 March 2019

Nagra, G., Treble, P. C., Andersen, M. S., Bajo, P., Hellstrom, J., and Baker, A.: Dating stalagmites in mediterranean climates using annual trace element cycles, Scientific Reports, 7, https://doi.org/10.1038/s41598-017-00474-4, 2017.

Noone, D., and Simmonds, I.: Associations between δ18O of Water and Climate Parameters in a Simulation of Atmospheric Circulation for 1979–95, Journal of Climate, 15, 3150-3169, https://doi.org/10.1175/1520-0442(2002)015<3150:aboowa>2.0.co;2, 2002.

Novello, V. F., Cruz, F. W., Vuille, M., Stríkis, N. M., Edwards, R. L., Cheng, H., Emerick, S., de Paula, M. S., Li, X., Barreto, E. d. S., Karmann, I., and Santos, R. V.: A high-resolution history of the South American Monsoon from Last Glacial Maximum to the Holocene, Scientific Reports, 7, 44267-44267, https://doi.org/10.1038/srep44267, 2017.

Novello, V. F., Cruz, F. W., Moquet, J. S., Vuille, M., de Paula, M. S., Nunes, D., Edwards, R. L., Cheng, H., Karmann, I., Utida, G., Stríkis, N. M., and Campos, J. L. P. S.: Two Millennia of South Atlantic Convergence Zone Variability Reconstructed From Isotopic Proxies, Geophysical Research Letters, 45, 5045-5051, https://doi.org/10.1029/2017GL076838, 2018.

Oster, J. L., Montañez, I. P., Mertz-Kraus, R., Sharp, W. D., Stock, G. M., Spero, H. J., Tinsley, J., and Zachos, J. C.: Millennial-scale variations in western Sierra Nevada precipitation during the last glacial cycle MIS 4/3 transition, Quaternary Research, 82, 236-248, https://doi.org/10.1016/j.yqres.2014.04.010, 2014.

Oster, J. L., Sharp, W. D., Covey, A. K., Gibson, J., Rogers, B., and Mix, H.: Climate response to the 8.2 ka event in coastal California, Scientific Reports, 7, 3886-3886, https://doi.org/10.1038/s41598-017-04215-5, 2017.

Partin, J. W., Cobb, K. M., Adkins, J. F., Clark, B., and Fernandez, D. P.: Millennial-scale trends in west Pacific warm pool hydrology since the Last Glacial Maximum, Nature, 449, 452-455, https://doi.org/10.1038/nature06164, 2007.

Paul, A., and Schäfer-Neth, C.: Modeling the water masses of the Atlantic Ocean at the Last Glacial Maximum, Paleoceanography, 18, https://doi.org/10.1029/2002PA000783, 2003.

Perez-Sanz, A., Li, G., González-Sampériz, P., and Harrison, S. P.: Evaluation of modern and mid-Holocene seasonal precipitation of the Mediterranean and northern Africa in the CMIP5 simulations, Clim. Past, 10, 551-568, https://doi.org/10.5194/cp-10-551-2014, 2014.

Pollock, A. L., van Beynen, P. E., DeLong, K. L., Polyak, V., Asmerom, Y., and Reeder, P. P.: A mid-Holocene paleoprecipitation record from Belize, Palaeogeography, Palaeoclimatology, Palaeoecology, 463, 103-111, https://doi.org/10.1016/J.PALAEO.2016.09.021, 2016.

Prentice, I. C., Cleator, S. F., Huang, Y. H., Harrison, S. P., and Roulstone, I.: Reconstructing ice-age palaeoclimates: Quantifying low-CO2 effects on plants, Global and Planetary Change, 149, 166-176, https://doi.org/10.1016/j.gloplacha.2016.12.012, 2017.

Riechelmann, S., Schroder-Ritzrau, A., Spotl, C., Riechelmann, D. F. C., Richter, D. K., Mangini, A., Frank, N., Breitenbach, S. F. M., and Immenhauser, A.: Sensitivity of Bunker Cave to climatic forcings highlighted through multi-annual monitoring of rain-, soil-, and dripwaters, Chemical Geology, 449, 194-205, https://doi.org/10.1016/j.chemgeo.2016.12.015, 2017.

Risi, C., Ogée, J., Bony, S., Bariac, T., Raz-Yaseef, N., Wingate, L., Welker, J., Knohl, A., Kurz-Besson, C., Leclerc, M., Zhang, G., Buchmann, N., Santrucek, J., Hronkova, M., David, T., Peylin, P., and Guglielmo, F.: The Water Isotopic Version of the Land-Surface Model ORCHIDEE: Implementation, Evaluation, Sensitivity to Hydrological Parameters, Hydrology: Current Research, 7, https://doi.org/10.4172/2157-7587.1000258, 2016.

Roche, D. M.: δ18O water isotope in the iLOVECLIM model (version 1.0) – Part 1: Implementation and verification, Geosci. Model Dev., 6, 1481-1491, https://doi.org/10.5194/gmd-6-1481-2013, 2013.

Roeckner, E., Baeuml, G., Bonaventura, L., Brokopf, R., Esch, M., Giorgetta, M., Hagemann, S., Kirchner, I., Kornblueh, L., Manzini, E., Rhodin, A., Schlese, U., Schulzweida, U., and Tompkins, A.: The general circulation model ECHAM5. Part I: Model description, Max Planck Institute for Meteorology, Hamburg 349, 140, 2003.

Roeckner, E., Brokopf, R., Esch, M., Giorgetta, M., Hagemann, S., Kornblueh, L., Manzini, E., Schlese, U., and Schulzweida, U.: Sensitivity of Simulated Climate to Horizontal and Vertical Resolution in the ECHAM5 Atmosphere Model, Journal of Climate, 19, 3771-3791, https://doi.org/10.1175/jcli3824.1, 2006.

Rowe, P. J., Mason, J. E., Andrews, J. E., Marca, A. D., Thomas, L., van Calsteren, P., Jex, C. N., Vonhof, H. B., and Al-Omari, S.: Speleothem isotopic evidence of winter rainfall variability in northeast Turkey between 77 and 6 ka, Quaternary Science Reviews, 45, 60-72, https://doi.org/10.1016/J.QUASCIREV.2012.04.013, 2012.

Schmidt, G. A., LeGrande, A. N., and Hoffmann, G.: Water isotope expressions of intrinsic and forced variability in a coupled ocean-atmosphere model, Journal of Geophysical Research: Atmospheres, 112, https://doi.org/10.1029/2006JD007781, 2007.

Schmidt, G. A., Annan, J. D., Bartlein, P. J., Cook, B. I., Guilyardi, E., Hargreaves, J. C., Harrison, S. P., Kageyama, M., LeGrande, A. N., Konecky, B., Lovejoy, S., Mann, M. E., Masson-Delmotte, V., Risi, C., Thompson, D., Timmermann, A., Tremblay, L. B., and Yiou, P.: Using palaeo-climate comparisons to constrain future projections in CMIP5, Clim. Past, 10, 221-250, https://doi.org/10.5194/cp-10-221-2014, 2014.

Scroxton, N., Gagan, M. K., Dunbar, G. B., Ayliffe, L. K., Hantoro, W. S., Shen, C.-C., Hellstrom, J. C., Zhao, J.-x., Cheng, H., Edwards, R. L., Sun, H., and Rifai, H.: Natural attrition and growth frequency variations of stalagmites in southwest Sulawesi over the past 530,000years, Palaeogeography, Palaeoclimatology, Palaeoecology, 441, 823-833, https://doi.org/10.1016/j.palaeo.2015.10.030, 2016.

Sharp, Z.: Principles of stable isotope geochemistry, 1st ed., Pearson Education, Upper Saddler River, N.J., 2007.

Stinnesbeck, W., Becker, J., Hering, F., Frey, E., Gonzalez, A. G., Fohlmeister, J., Stinnesbeck, S., Frank, N., Mata, A. T., Benavente, M. E., Olguin, J. A., Nunez, E. A., Zell, P., and Deininger, M.: The earliest settlers of Mesoamerica date back to the late Pleistocene, Plos One, 12, https://doi.org/10.1371/journal.pone.0183345, 2017.

Sundqvist, H. S., Holmgren, K., and Lauritzen, S. E.: Stable isotope variations in stalagmites from northwestern Sweden document climate and environmental changes during the early Holocene, The Holocene, 17, 259-267, https://doi.org/10.1177/0959683607073292, 2007.

Tindall, J. C., Valdes, P. J., and Sime, L. C.: Stable water isotopes in HadCM3: Isotopic signature of El Niño–Southern Oscillation and the tropical amount effect, Journal of Geophysical Research: Atmospheres, 114, https://doi.org/10.1029/2008JD010825, 2009.

Treble, P., Shelley, J. M. G., and Chappell, J.: Comparison of high resolution sub-annual records of trace elements in a modern (1911–1992) speleothem with instrumental climate data from southwest Australia, Earth and Planetary Science Letters, 216, 141-153, https://doi.org/10.1016/S0012-821X(03)00504-1, 2003.

Treble, P. C., Chappell, J., Gagan, M. K., McKeegan, K. D., and Harrison, T. M.: In situ measurement of seasonal delta O-18 variations and analysis of isotopic trends in a modem speleothem from southwest Australia, Earth and Planetary Science Letters, 233, 17-32, https://doi.org/10.1016/j.epsl.2005.02.013, 2005.

Treble, P. C., Baker, A., Ayliffe, L. K., Cohen, T. J., Hellstrom, J. C., Gagan, M. K., Frisia, S., Drysdale, R. N., Griffiths, A. D., and Borsato, A.: Hydroclimate of the Last Glacial Maximum and deglaciation in southern Australia's arid margin interpreted from speleothem records (23-15 ka), Climate of the Past, 13, 667-687, https://doi.org/10.5194/cp-13-667-2017, 2017.

Tremaine, D. M., Froelich, P. N., and Wang, Y.: Speleothem calcite farmed in situ: Modern calibration of δ18O and δ13C paleoclimate proxies in a continuously-monitored natural cave system, Geochimica et Cosmochimica Acta, 75, 4929-4950, https://doi.org/10.1016/j.gca.2011.06.005, 2011.

Vaks, A., Bar-Matthews, M., Ayalon, A., Matthews, A., Frumkin, A., Dayan, U., Halicz, L., Almogi-Labin, A., and Schilman, B.: Paleoclimate and location of the border between Mediterranean climate region and the Saharo-Arabian Desert as revealed by speleothems from the northern Negev Desert, Israel, Earth and Planetary Science Letters, 249, 384-399, https://doi.org/10.1016/j.epsl.2006.07.009, 2006.

Vaks, A., Gutareva, O. S., Breitenbach, S. F. M., Avirmed, E., Mason, A. J., Thomas, A. L., Osinzev, A. V., Kononov, A. M., and Henderson, G. M.: Speleothems Reveal 500,000-Year History of Siberian Permafrost, Science, 340, 183-186, https://doi.org/10.1126/science.1228729, 2013.

Vanghi, V., Borsato, A., Frisia, S., Drysdale, R., Hellstrom, J., and Bajo, P.: Climate variability on the Adriatic seaboard during the last glacial inception and MIS 5c from Frasassi Cave stalagmite record, Quaternary Science Reviews, 201, 349-361, https://doi.org/10.1016/J.QUASCIREV.2018.10.023, 2018.

Wackerbarth, A., Langebroek, P. M., Werner, M., Lohmann, G., Riechelmann, S., Borsato, A., and Mangini, A.: Simulated oxygen isotopes in cave drip water and speleothem calcite in

Clim. Past Discuss., https://doi.org/10.5194/cp-2019-25
Manuscript under review for journal Clim. Past
Discussion started: 4 March 2019

Climate of the Past
Discussions
Open Access

European caves, Climate of the Past, 8, 1781-1799, https://doi.org/10.5194/cp-8-1781-2012, 2012.

Wang, X., Edwards, R. L., Auler, A. S., Cheng, H., Kong, X., Wang, Y., Cruz, F. W., Dorale, J. A., and Chiang, H.-W.: Hydroclimate changes across the Amazon lowlands over the past 45,000 years, Nature, 541, 204-207, https://doi.org/10.1038/nature20787, 2017.

Wang, Y., Cheng, H., Edwards, R. L., He, Y., Kong, X., An, Z., Wu, J., Kelly, M. J., Dykoski, C. A., and Li, X.: The Holocene Asian monsoon: links to solar changes and North Atlantic climate, Science (New York, N.Y.), 308, 854-857, https://doi.org/10.1126/science.1106296, 2005.

Waterisotopes Database: http://waterisotopes.org Accessed 04/2017. Query: type=Precipitation, 2017.

Werner, M., Langebroek, P. M., Carlsen, T., Herold, M., and Lohmann, G.: Stable water isotopes in the ECHAM5 general circulation model: Toward high-resolution isotope modeling on a global scale, Journal of Geophysical Research: Atmospheres, 116, https://doi.org/10.1029/2011JD015681, 2011.

Werner, M., Haese, B., Xu, X., Zhang, X., Butzin, M., and Lohmann, G.: Glacial-interglacial changes in (H2O)-O-18, HDO and deuterium excess - results from the fully coupled ECHAM5/MPI-OM Earth system model, Geoscientific Model Development, 9, 647-670, https://doi.org/10.5194/gmd-9-647-2016, 2016.

Werner, M., Jouzel, J., Masson-Delmotte, V., and Lohmann, G.: Reconciling glacial Antarctic water stable isotopes with ice sheet topography and the isotopic paleothermometer, Nature Communications, 9, 3537, https://doi.org/10.1038/s41467-018-05430-y, 2018.

Winter, A., Zanchettin, D., Miller, T., Kushnir, Y., Black, D., Lohmann, G., Burnett, A., Haug, G. H., Estrella-Martínez, J., Breitenbach, S. F. M., Beaufort, L., Rubino, A., and Cheng, H.: Persistent drying in the tropics linked to natural forcing, Nature Communications, 6, 7627-7627, https://doi.org/10.1038/ncomms8627, 2015.

Wolff, C., Plessen, B., Dudashvilli, A. S., Breitenbach, S. F., Cheng, H., Edwards, L. R., and Strecker, M. R.: Precipitation evolution of Central Asia during the last 5000 years, Holocene, 27, 142-154, https://doi.org/10.1177/0959683616652711, 2017.

Wurtzel, J. B., Abram, N. J., Lewis, S. C., Bajo, P., Hellstrom, J. C., Troitzsch, U., and Heslop, D.: Tropical Indo-Pacific hydroclimate response to North Atlantic forcing during the last deglaciation as recorded by a speleothem from Sumatra, Indonesia, Earth and Planetary Science Letters, 492, 264-278, https://doi.org/10.1016/J.EPSL.2018.04.001, 2018.

Xi, X.: A Review of Water Isotopes in Atmospheric General Circulation Models: Recent Advances and Future Prospects, International Journal of Atmospheric Sciences, 2014, 16, https://doi.org/10.1155/2014/250920, 2014.

Xia, Q. K., Zhao, J. X., and Collerson, K. D.: Early-Mid Holocene climatic variations in Tasmania, Australia: multi-proxy records in a stalagmite from Lynds Cave, Earth and Planetary Science Letters, 194, 177-187, https://doi.org/10.1016/s0012-821x(01)00541-6, 2001.

Zhu, J., Liu, Z. Y., Brady, E. C., Otto-Bliesner, B. L., Marcott, S. A., Zhang, J. X., Wang, X. F., Nusbaumer, J., Wong, T. E., Jahn, A., and Noone, D.: Investigating the Direct Meltwater Effect in Terrestrial Oxygen-Isotope Paleoclimate Records Using an Isotope-Enabled Earth System Model, Geophysical Research Letters, 44, 12501-12510, https://doi.org/10.1002/2017gl076253, 2017.

Clim. Past Discuss., https://doi.org/10.5194/cp-2019-25
Manuscript under review for journal Clim. Past
Discussion started: 4 March 2019

Climate of the Past Discussions
Open Access

Figure Captions

Figure 1: Spatio-temporal distribution of SISALv1b database. **(a)** Spatial distribution of speleothem records. Filled circles are sites used in this study (SISALv1 in purple; SISALv1b in light blue). Crosses are SISAL sites that do not pass the screening described in section 2.3 and/or do not cover the time periods used here (modern, MH and LGM). The background carbonate lithology is that of the World Karst Aquifer Mapping (WOKAM) project (Chen et al., 2017). **(b)** Temporal distribution of speleothem records according to regions. The non-overlapping bins span 1,000 years and start on 1950 CE. Regions have been defined as: Oceania (-60° < Lat < 0°; 90° < Lon < 180°); Asia (0° < Lat < 60°; 60° < Lon < 130°); Middle East (7.6° < Lat < 50°; 26° < Lon < 59°); Africa (-45° < Lat < 36.1°; -30° < Lon < 60°; with records in the Middle East region removed); Europe (36.7° < Lat < 75°; -30° < Lon < 30°; plus Gibraltar and Siberian sites); South America (-60° < Lat < 8°; -150° < Lon < -30°); North and Central America (8.1° < Lat < 60°; -150° < Lon < -50°).

Figure 2: Distribution of the number of unique caves with speleothem growth through time. (**a)** Number of unique caves with growth over the last 500 yrs BP in 1000-year bins (solid line), bootstrapped estimate of uncertainty (shading between 5 and 95% percentiles) and fitted exponential distribution (darker solid line). (**b, c**) same as a) but with the fitted exponential distribution subtracted to highlight anomalies from the expected number of caves over the last 300 kyrs BP. Horizontal bars in b) and c) indicate periods with significantly greater (dark grey) or fewer (light grey) number of caves with speleothem growth than expected. Green indicates the full global dataset, blue and red indicate temperate and tropical subdivisions respectively. Horizontal bars in a) denote previous interglacials.

Figure 3: Comparison of SISAL data with observational and simulated w$\delta^{18}O_p$ for the modern period. **(a)** Comparison between SISAL $\delta^{18}O$ averages [‰; V-SMOW] for the period 1960–2017 with OIPC data [‰; V-SMOW]. **(b)** Scatterplot of SISAL modern $\delta^{18}O$ averages as in (a) versus w$\delta^{18}O_p$ extracted from OIPC (i.e., background map in (a)) at the location of each cave site. **(c)** Same than (a) with simulated w$\delta^{18}O_p$ data for the period 1958–2013 in the background. **(d)** Scatterplot of SISAL

modern δ^{18}O as in (c) versus the simulated wδ$^{18}O_p$ for the period 1958–2013. Dashed lines in (b) and (d) represents the 1:1 line. All SISAL isotope data have been converted to their drip-water equivalent using the calcite-water δ^{18}O fractionation equation from Tremaine et al. (2011). Mean annual air surface temperature from CRU-TS4.01 (Harris et al., 2014) and mean annual simulated ECHAM5-wiso air surface temperature were used as surrogates for cave temperatures in the OIPC and ECHAM5-wiso comparison, respectively. See section 2.3 for details on data extraction and conversion.

Figure 4: Modern global inter-annual δ^{18}O variability. Box plots show the variability of the standard deviation of global annual δ^{18}O using: **(left)** GNIP stations with at least 10 months of data per year and at least 5 years of data (n = 450) and ECHAM5-wiso data extracted at the location of each GNIP station for the years when this data is available; **(right)** SISAL records with at least 5 isotope samples for the period 1958–2013 and simulated wδ$^{18}O_p$ extracted at each cave location for the same years for which speleothem data is available. Boxplots in shades of red at the rightmost of the panel are constructed after smoothing the simulated wδ$^{18}O_p$ data for 1 to 16 years . On each box, the central red mark indicates the median (q_2; 50th percentile) and the bottom and top edges of the box indicate the 25th (q_1) and 75th (q_3) percentiles, respectively. Outliers (red crosses) are locations with standard deviations greater than $q_3 + 1.5 \times (q_3 - q_1)$ or less than $q_1 - 1.5 \times (q_3 - q_1)$. This corresponds to approximately ±2.7σ or 99.3% coverage if the data are normally distributed. If the notches in the box plots do not overlap, you can conclude, with 95% confidence, that the true medians do differ. The grey horizontal band corresponds to the notch in SISAL for easy comparison. SISAL were converted to their drip-water δ^{18}O equivalent as described in section 2.3.

Figure 5: ECHAM5-wiso weighted δ$^{18}O_p$ anomalies ([‰; V-SMOW]; background map) and SISAL isotope anomalies ([‰; V-PDB]; filled circles) for three time-slices: **(a)** MH-PI (SISAL records n = 34), **(b)** LGM-PI (SISAL records n = 11) and **(c)** LGM-MH (SISAL records n = 20). For easy visualisation, when there are two speleothem records from the same cave site, one has been shifted 2^{o} towards the North and the East (shown here as triangles). Note the different colour bar axis in the colour bar of (a)

compared to (b) and (c). Two-tailed student t-test has been applied to calculate the significance of the ECHAM5-wiso anomalies in (a) and (b) at a 95% confidence. No significance has been calculated for (c), which compares two different simulations with their corresponding control periods. SISAL anomalies calculated with respect to 1850–1990. SISAL data has been converted to its drip water equivalent prior to calculating the anomalies.

Figure 6: LGM period definitions and their impact on SISAL $\delta^{18}O$ mean estimate uncertainty. The impact of the window definition and age uncertainty is explored for two entities **(a)** entity BT-2 from Botuverá cave (Cruz et al., 2005)and **(b)** entity SSC01 from Gunung-buda cave (Partin et al., 2007). The relative error is defined as 2 standard deviations for the original age model and the COPRA median; and the upper minus lower 95% quantiles for the COPRA median uncertainty as well as the COPRA ensemble spread of standard deviations. Black solid lines give the relative error of the mean isotopic estimate for the LGM for the original age model, the grey solid line for the estimate based on the COPRA median age model. The pink dotted line shows the uncertainty of the COPRA median estimate, and the green dashed line the average relative error estimate across the 1,000-member COPRA ensemble. For both speleothems, relatively stable error estimates are found for window sizes larger than 750 years, whereas the relative error increases towards smaller window sizes.

Figure 7: Mid-Holocene (MH) transects for three regions: **(a)** NW to SE across North America; **(b)** N-S across southern Europe and northern Africa, and **(c)** NW to SE across SE Asia. Maps at the top of each panel show the simulated $\delta^{18}O_p$ (left), Mean Annual Temperature (MAT; centre) and Mean Annual Precipitation (MAP; right) from ECHAM5-wiso. The same scale is used for the $\delta^{18}O$, MAT and MAP maps. All transects show absolute $\delta^{18}O$ values. In the $\delta^{18}O$ maps, filled circles are SISAL $\delta^{18}O$ averages for entities that cover both the MH and the modern reference period. Filled squares are SISAL entities that do not have a corresponding modern. Bottom plots of each panel show the simulated data extracted for each transect: black circles and whiskers are mean ±1 standard deviation of the data extracted along longitudinal sections in between the two great circle lines shown in solid

grey lines in the top maps. The red line is the median of the extracted data. All data were extracted at steps of 1.12° to coincide with the average model grid-size. Bottom plots in each panel also show SISAL $\delta^{18}O$ (circles for low-elevation sites, < 1,000 masl; triangles for high-elevation sites, > 1,000 masl), pollen-based quantitative reconstructions of MAT (red squares; Bartlein et al., 2011) and MAP (blue squares; Bartlein et al., 2011). Pollen-based reconstructions have been converted to absolute values by adding the CRU-TS4.01 climatology (Harris et al., 2014).

Figure 8: Last Glacial Maximum (LGM) transects for three regions: **(a)** NW to SE across North America; **(b)** N-S from central Europe to southern Africa, and **(c)** NW-SE from China to northern Australia. Details as in caption of Fig. 7.

Table Captions

Table 1: List of speleothem records that have been added to SISALv1 (Atsawawaranunt et al., 2018a;Atsawawaranunt et al., 2018b) to produce SISALv1b (Atsawawaranunt et al., 2019) sorted alphabetically by site name. Elevation is in metres above sea level (masl), latitude in degrees North and longitude in degrees East.

Table 2: Number of SISALv1b speleothem records available for key time periods. Mid-Holocene (MH): 6±0.5 kyrs BP; Last Glacial Maximum (LGM): 21±1 kyrs BP. “kyrs BP” refers to thousand years before present, where present is 1950 CE.

Climate of the Past
Discussions
Open Access

1185 **Figure 1**

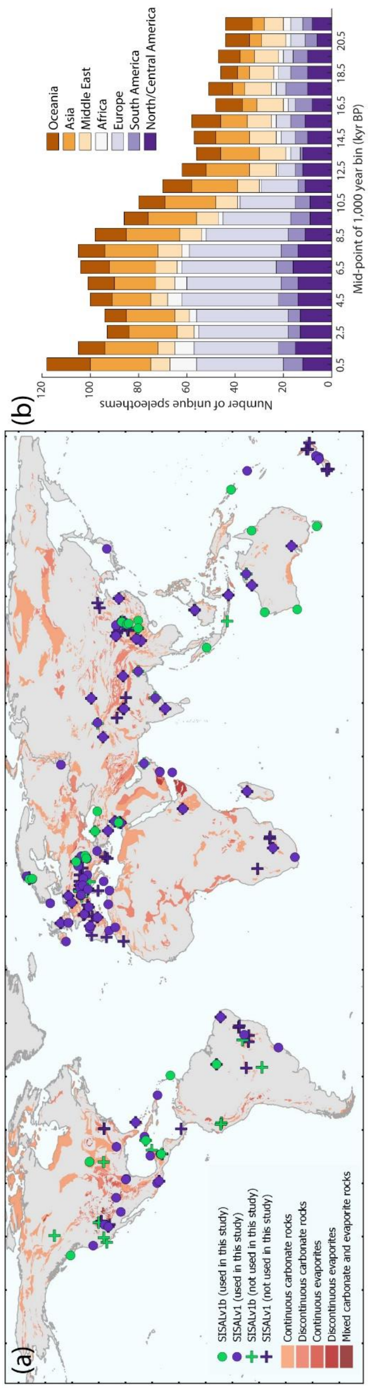

Clim. Past Discuss., https://doi.org/10.5194/cp-2019-25
Manuscript under review for journal Clim. Past
Discussion started: 4 March 2019

Climate of the Past Discussions
Open Access
EGU

1186 **Figure 2**

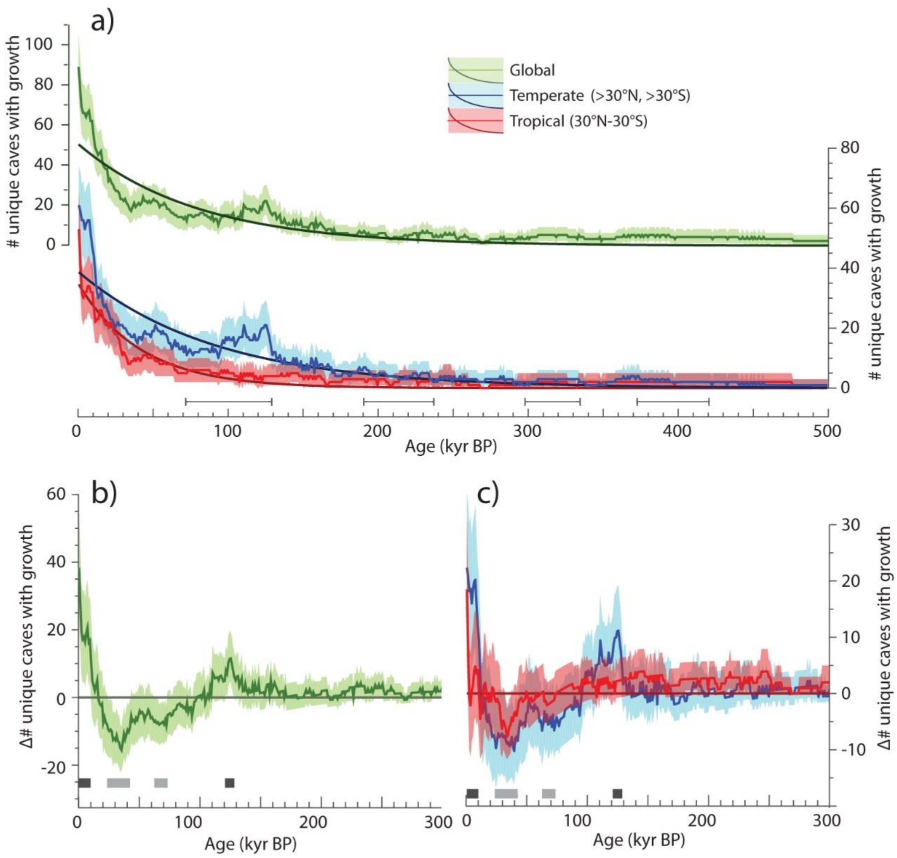

1187 **Figure 3**

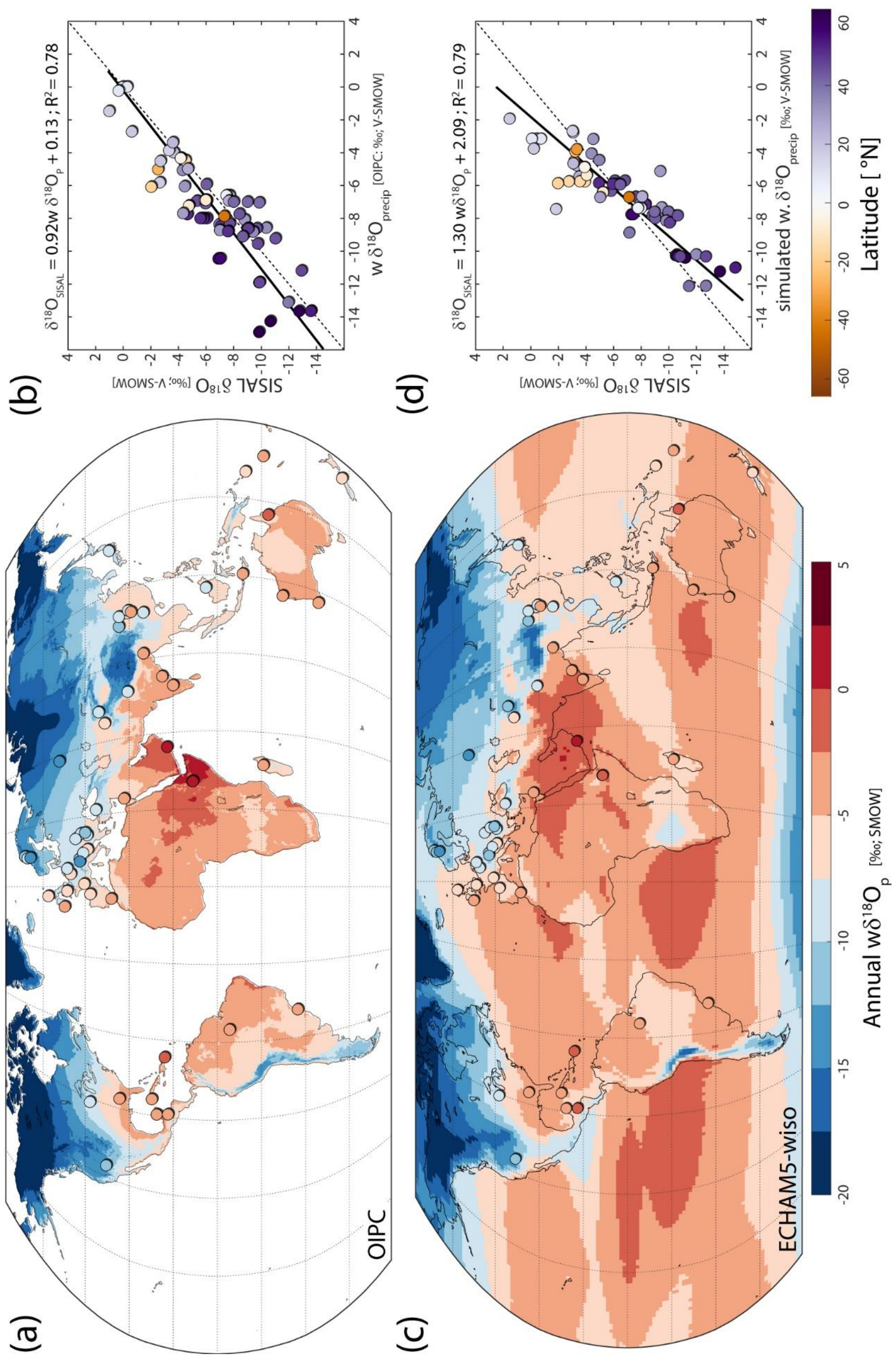

Clim. Past Discuss., https://doi.org/10.5194/cp-2019-25
Manuscript under review for journal Clim. Past
Discussion started: 4 March 2019

1188 **Figure 4**

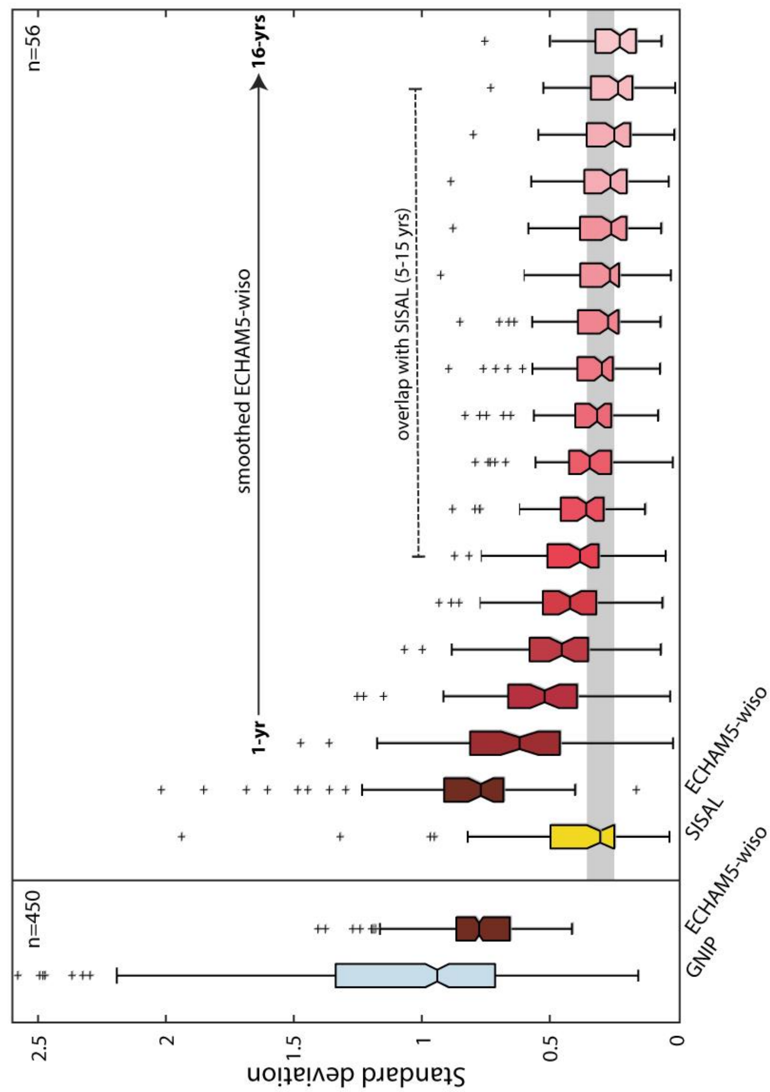

Clim. Past Discuss., https://doi.org/10.5194/cp-2019-25
Manuscript under review for journal Clim. Past
Discussion started: 4 March 2019

Climate of the Past Discussions

1189 **Figure 5**

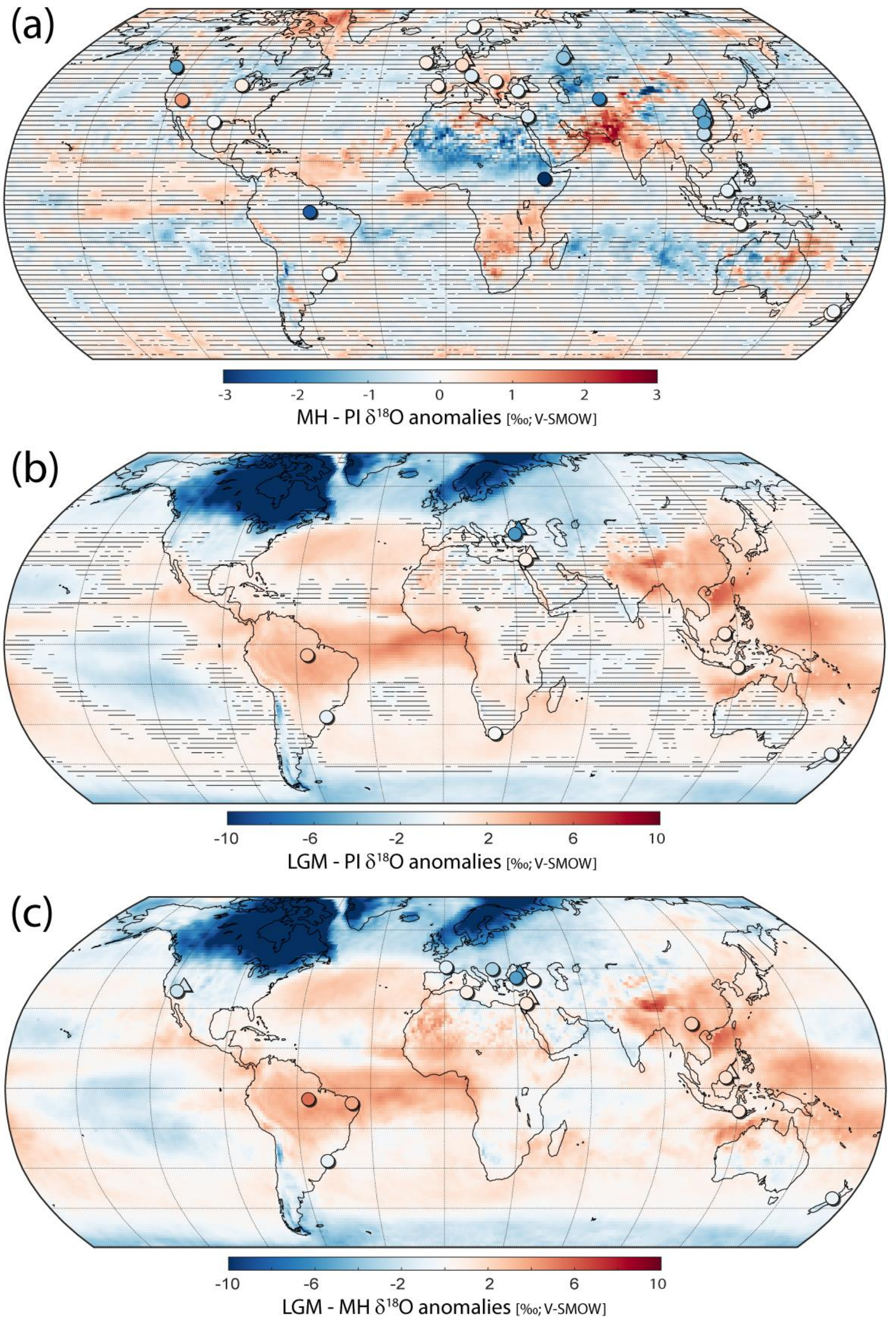

Clim. Past Discuss., https://doi.org/10.5194/cp-2019-25
Manuscript under review for journal Clim. Past
Discussion started: 4 March 2019

Climate of the Past Discussions
Open Access
EGU

1190 **Figure 6**

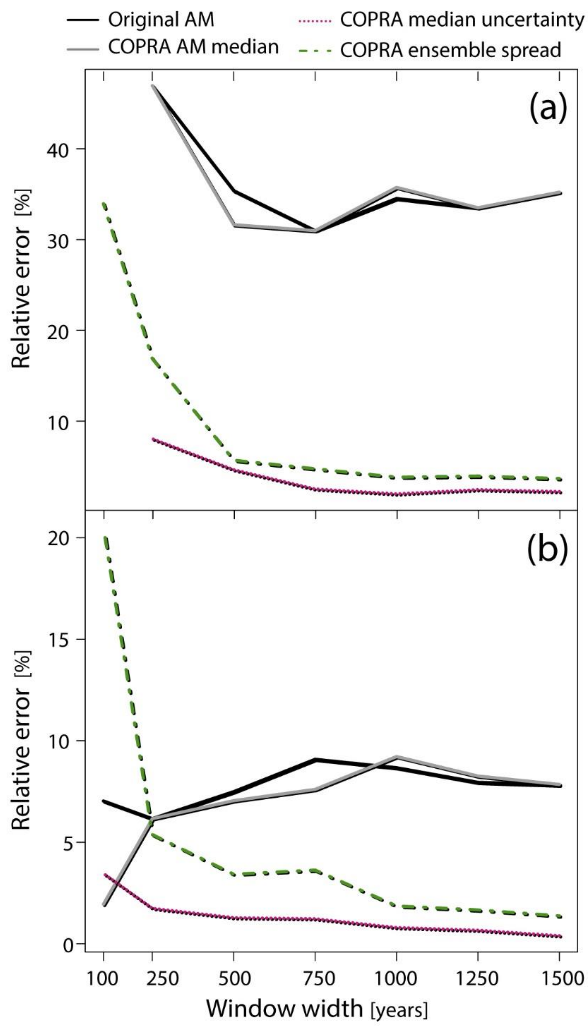

Clim. Past Discuss., https://doi.org/10.5194/cp-2019-25
Manuscript under review for journal Clim. Past
Discussion started: 4 March 2019

Climate of the Past Discussions

1191 **Figure 7**

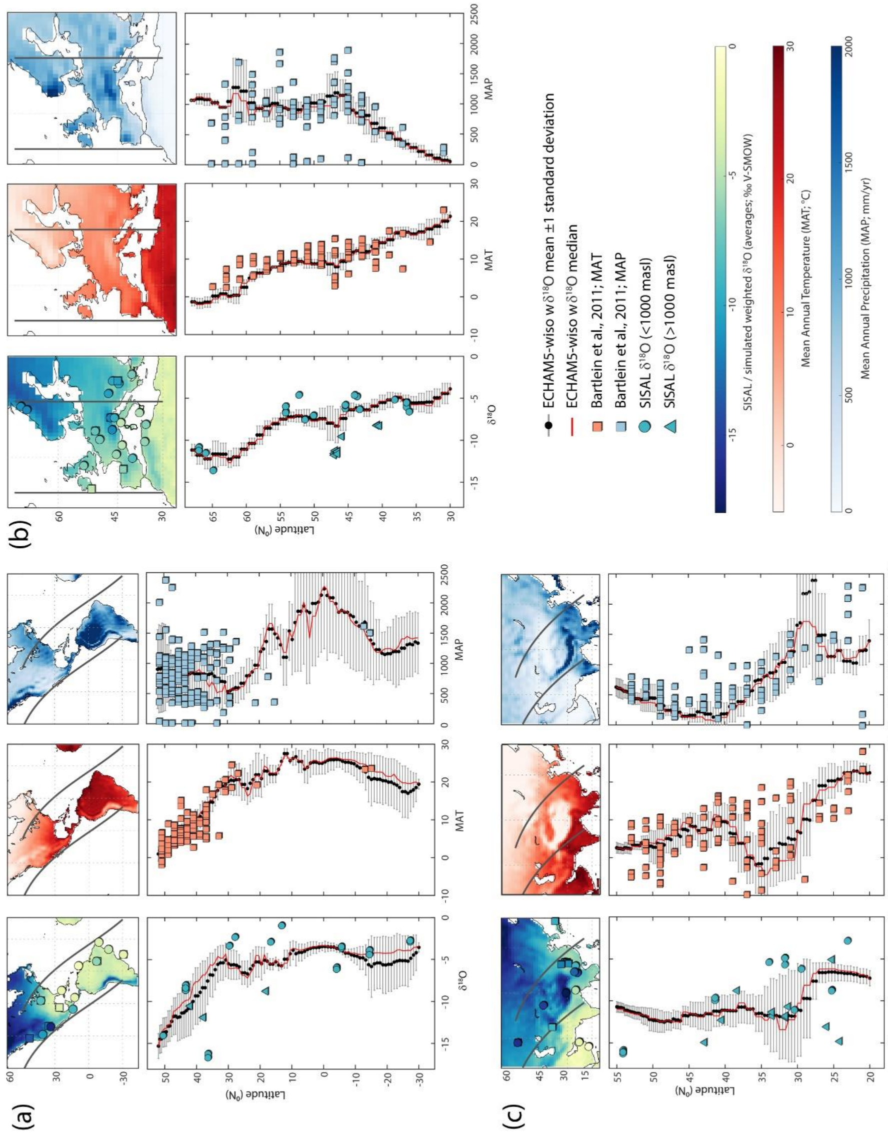

Clim. Past Discuss., https://doi.org/10.5194/cp-2019-25
Manuscript under review for journal Clim. Past
Discussion started: 4 March 2019

Climate of the Past
Discussions

Figure 8

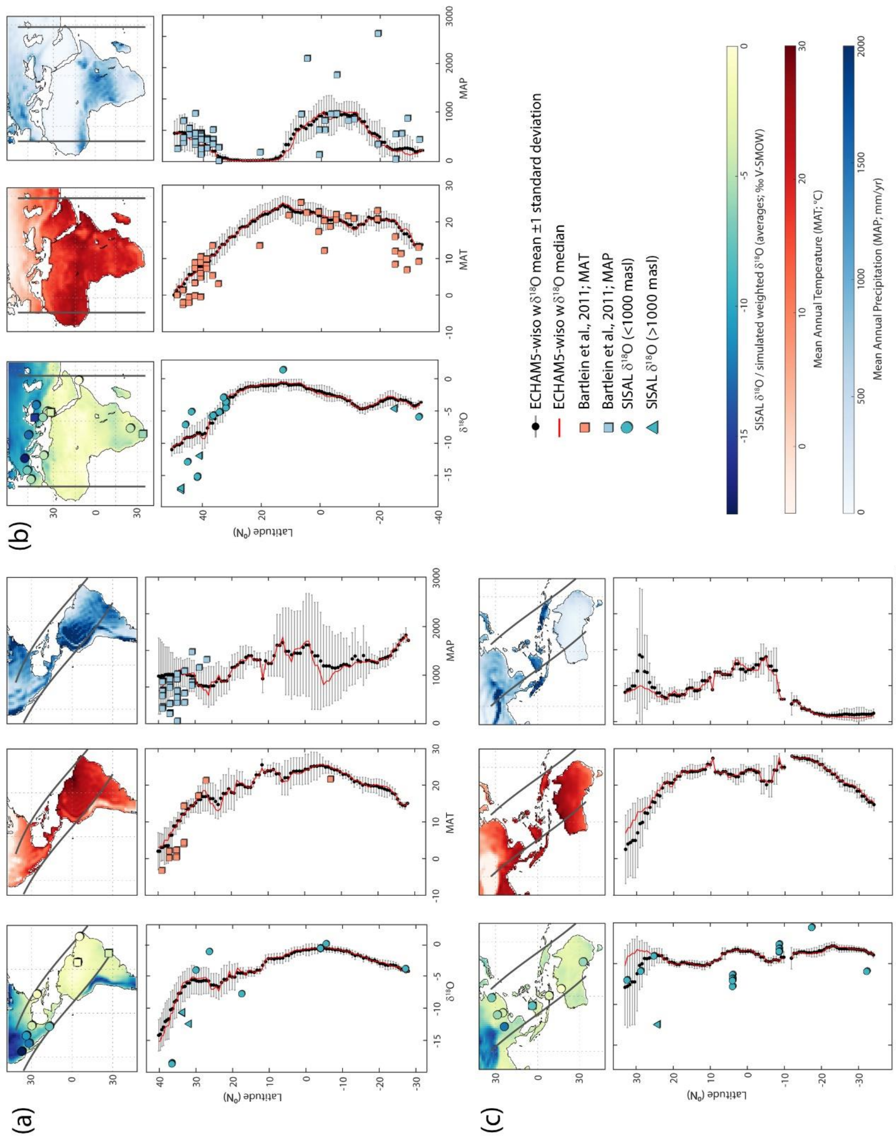

1194 **Table 1:**

Site name	Elev.	Lat.	Lon.	Entity name	Reference (s)
Arch cave	660	50.55	-127.07	DM05-01	Marshall et al. (2009)
Beatus cave	875	46.38	7.49	EXC3, EXC4	Boch et al. (2011)
Bribin cave	500	-8.05	110.633	JB2	Hartmann et al. (2013)
Cesare Battisti cave	1880	46.08	11.02	CB25, CB39, CB47	Johnston et al. (2018)
Chan Hol cave	-8.5	20.16	-87.57	CH-7	Stinnesbeck et al. (2017)
Chen Ha cave	550	16.6769	-89.0925	CH04-02	Pollock et al. (2016)
Cold Water cave	356	43.4678	-91.975	CWC-1s, CWC-2ss, CWC-3l	Denniston et al. (1999)
Devil's Icebox cave	250	38.15	-92.05	DIB-1, DIB-2	Denniston et al. (2007b)
Dongge cave	680	25.2833	108.0833	DA_2005, D4_2005	Wang et al. (2005);Dykoski et al. (2005)
Dos Anas cave	120	22.38	-83.97	CG	Fensterer et al. (2010);Fensterer et al. (2012)
El Condor cave	860	-5.93	-77.3	ELC_composite	Cheng et al. (2013)
Frasassi cave system - Grotta Grande del Vento	257	43.4008	12.9619	FR16	Vanghi et al. (2018)
Goshute cave	2000	40.0333	-114.783	GC_2, GC_3	Denniston et al. (2007a)
Harrison's cave	300	13.2	-59.6	HC-1	Mangini et al. (2007);Mickler et al. (2004);Mickler et al. (2006)
Hoti cave	800	23.0833	57.35	H14	Cheng et al. (2009);Fleitmann et al. (2003)
Jaraguá cave	570	-21.083	-56.583	JAR4, JAR1, JAR_composite	Novello et al. (2018);Novello et al. (2017)
Karaca cave	1536	40.5443	39.4029	K1	Rowe et al. (2012)
Klaus Cramer cave	1964	47.26	9.52	KC1	Boch et al. (2011)
KNI-51 cave	100	-15.18	128.37	KNI-51-A1, KNI-51-P	Denniston et al. (2013)
Korallgrottan cave	570	64.88	14.15	K1	Sundqvist et al. (2007)
Lianhua	455	29.48	109.53	A1	Cosford et al. (2008a)
Lynds cave	300	-41.58	146.25	Lynds_BCD	Xia et al. (2001)
Mawmluh cave	1160	25.2622	91.8817	MAW-0201	Myers et al. (2015)
McLean's cave	300	38.07	-120.42	ML2	Oster et al. (2014)
Minnetonka cave	2347	56.5833	-119.65	MC08-1	Lundeen et al. (2013)
Moondyne cave	100	-34.27	115.08	MND-S1	Fischer and Treble (2008);Nagra et al. (2017) Treble et al. (2003);Treble et al. (2005)

Paraiso cave	60	-4.0667	-55.45	Paraiso composite	Wang et al. (2017)
Peqiin cave	650	32.58	35.19	PEK_composite, PEK 6, PEK 9, PEK 10	Bar-Matthews et al. (2003)
Piani Eterni karst system	1893	46.16	11.99	MN1, GG1, IS1	Columbu et al. (2018)
Poleva cave	390	44.7144	21.7469	PP10	Constantin et al. (2007)
São Bernardo cave	631	-13.81	-46.35	SBE3	Novello et al. (2018)
São Matheus cave	631	-13.81	-46.35	SMT5	Novello et al. (2018)
Shatuca cave	1960	-5.7	-77.9	Sha-2, Sha-3, Sha-composite	Bustamante et al. (2016)
Sofular cave	440	41.42	31.93	So-17A, So-2	Badertscher et al. (2011);Fleitmann et al. (2009) Göktürk et al. (2011)
Soylegrotta cave	280	66	14	SG93	Lauritzen and Lundberg (1999)
Tangga cave	600	-0.36	100.76	TA12-2	Wurtzel et al. (2018)
Uluu-Too cave	1490	40.4	72.35	Uluu2	Wolff et al. (2017)
White moon cave	170	37	-122.183	WMC1	Oster et al. (2017)
Xiangshui cave	380	25.25	110.92	X3	Cosford et al. (2008b)
Xibalba cave	350	16.5	-89	GU-Xi-1	Winter et al. (2015)
Yaoba Don cave	420	28.8	109.83	YB	Cosford et al. (2008b)

1195 **Table 2:**

Time period	**Number of speleothems (entities) and cave sites in both periods**
Modern (1961–1990 CE)	58 entities (47 sites)
PI (1835–1865 CE)	62 entities (51 sites)
Extended PI (1850–1990 CE)	87 entities (69 sites)
MH and PI	18 entities (17 sites)
MH and extended PI	34 entities (29 sites)
MH and Last Millennium (LM, 850–1850 CE)	48 entities (38 sites)
LGM and PI	5 entities (5 sites)
LGM and extended PI	11 entities (10 sites)
LGM and Last Millennium (LM, 850–1850 CE)	12 entities (10 sites)
LGM and MH	20 entities (16 sites)